Plant Physiology®

Plant Physiology, 2024, **196**, 1562–1578
https://doi.org/10.1093/plphys/kiae370
Advance access publication 8 July 2024
Research Article

Cell wall integrity modulates *HOOKLESS1* and *PHYTOCHROME INTERACTING FACTOR4* expression controlling apical hook formation

Riccardo Lorrai,[1] Özer Erguvan,[2] Sara Raggi,[2] Kristoffer Jonsson,[3] Jitka Široká,[4] Danuše Tarkowská,[4] Ondřej Novák,[4] Jayne Griffiths,[5] Alexander M. Jones,[5] Stéphane Verger,[2,6] Stéphanie Robert,[2] and Simone Ferrari[1,*]

[1]Dipartimento di Biologia e biotecnologie "Charles Darwin", Sapienza Università di Roma, 00185 Rome, Italy
[2]Umeå Plant Science Centre (UPSC), Department of Forest Genetics and Plant Physiology, Swedish University of Agricultural Sciences, 901 83 Umeå, Sweden
[3]IRBV, Department of Biological Sciences, University of Montreal, QC H1X 2B2 Montreal, Quebec, Canada
[4]Laboratory of Growth Regulators, Institute of Experimental Botany, Czech Academy of Sciences and Faculty of Science, Palacký University Olomouc, CZ-77900 Olomouc, Czech Republic
[5]Sainsbury Laboratory, University of Cambridge, CB2 1LR Cambridge, UK
[6]Umeå Plant Science Centre (UPSC), Department of Plant Physiology, Umeå University, 901 87 Umeå, Sweden
*Author for correspondence: simone.ferrari@uniroma1.it
The author responsible for distribution of materials integral to the findings presented in this article in accordance with the policy described in the Instructions for Authors (https://academic.oup.com/plphys/pages/General-Instructions) is: Simone Ferrari (simone.ferrari@uniroma1.it).

Abstract

Formation of the apical hook in etiolated dicot seedlings results from differential growth in the hypocotyl apex and is tightly controlled by environmental cues and hormones, among which auxin and gibberellins (GAs) play an important role. Cell expansion is tightly regulated by the cell wall, but whether and how feedback from this structure contributes to hook development are still unclear. Here, we show that etiolated seedlings of the Arabidopsis (*Arabidopsis thaliana*) *quasimodo2-1* (*qua2*) mutant, defective in pectin biosynthesis, display severe defects in apical hook formation and maintenance, accompanied by loss of asymmetric auxin maxima and differential cell expansion. Moreover, *qua2* seedlings show reduced expression of *HOOKLESS1* (*HLS1*) and *PHYTOCHROME INTERACTING FACTOR4* (*PIF4*), which are positive regulators of hook formation. Treatment of wild-type seedlings with the cellulose inhibitor isoxaben (isx) also prevents hook development and represses *HLS1* and *PIF4* expression. Exogenous GAs, loss of DELLA proteins, or *HLS1* overexpression partially restore hook development in *qua2* and isx-treated seedlings. Interestingly, increased agar concentration in the medium restores, both in *qua2* and isx-treated seedlings, hook formation, asymmetric auxin maxima, and *PIF4* and *HLS1* expression. Analyses of plants expressing a Förster resonance energy transfer-based GA sensor indicate that isx reduces accumulation of GAs in the apical hook region in a turgor-dependent manner. Lack of the cell wall integrity sensor THESEUS 1, which modulates turgor loss point, restores hook formation in *qua2* and isx-treated seedlings. We propose that turgor-dependent signals link changes in cell wall integrity to the PIF4-HLS1 signaling module to control differential cell elongation during hook formation.

Introduction

Etiolated seedlings of dicots form an apical hook to protect the meristems during soil emergence. Apical hook formation depends on the differential cell elongation on the opposite sides of the hypocotyl apex, causing the shoot to bend by 180° (Guzmán and Ecker 1990; Abbas et al. 2013). Like most plant developmental processes, hook formation is largely controlled by phytohormones including auxin (Abbas et al. 2013). Shortly after germination, the formation of an auxin response maximum restrains cell expansion on the concave side of the hook, leading to differential cell elongation and eventually shoot bending (Abbas et al. 2013). In Arabidopsis (*Arabidopsis thaliana*), hook formation is positively controlled by the master regulator HOOKLESS1 (HLS1; Guzmán and Ecker 1990; Lehman et al. 1996; Li et al. 2004; Zhang et al. 2018). HLS1 was reported to promote the asymmetric distribution of auxin between the concave and convex sides of the hypocotyl (Lehman et al. 1996) and to reduce the levels of AUXIN RESPONSE FACTOR 2 (ARF2), a repressor of auxin responses (Li et al. 2004). Both apical hook formation and *HLS1* expression are promoted by ethylene and gibberellins (Gas; Lehman et al. 1996; An et al. 2012) and negatively regulated by jasmonates (Song et al. 2014). Regulation of hook formation by GAs is mediated by the degradation of the key repressors DELLA proteins (Sun 2008). When GA levels are low, DELLAs promote the proteasome-mediated degradation of PHYTOCHROME INTERACTING FACTORS (PIFs; Li et al. 2016), a family of transcription factors that positively regulate the expression of *HLS1* (Zhang et al. 2018). In addition, DELLAs inhibit the activity of PIFs by sequestering their DNA recognition domain (de Lucas et al. 2008; Feng et al. 2008). On the other hand, jasmonates can repress hook formation by reducing *HLS1* expression (Zhang et al. 2014) and by repressing PIF function (Zhang et al. 2018). While hormonal signals

Received February 23, 2024. Accepted June 11, 2024.

coordinate hook development, their effects ultimately translate into changes in cellular properties, particularly the ability of the cell wall to yield to turgor pressure. Primary cell walls are complex and dynamic networks mainly composed of cellulose, hemicelluloses, and pectin (Cosgrove 2005). Increasing evidence indicates that changes in plant cell wall structural polysaccharides caused either by mutations in biosynthetic genes or by chemicals, like the cellulose inhibitor isoxaben (isx; Heim et al. 1990), impair cell wall integrity (CWI), leading to repression of cell expansion and induction of stress responses (Vaahtera et al. 2019). For instance, etiolated Arabidopsis seedlings with altered cellulose deposition display strongly reduced hypocotyl growth (Fagard et al. 2000) and accumulate high levels of jasmonates (Engelsdorf et al. 2018). Defects in pectin composition also restrict the growth of etiolated hypocotyls. Two Arabidopsis mutants defective for genes required for homogalacturonan (HG) biosynthesis, namely *QUASIMODO1* (*QUA1*), encoding a putative glycosyltransferase (Bouton et al. 2002), and *QUASIMODO2/TUMOROUS SHOOT DEVELOPMENT 2* (*QUA2/TSD2*), encoding a Golgi-localized pectin methyltransferase (Krupková et al. 2007; Mouille et al. 2007; Du et al. 2020), have defects in hypocotyl epidermis cell elongation and cell-to-cell adhesion (Krupková et al. 2007; Mouille et al. 2007; Raggi et al. 2015).

The molecular mechanisms regulating responses triggered by loss of CWI are only partly understood. Several responses triggered by cellulose alterations appear to be mediated by THESEUS 1 (THE1), a member of the *Catharanthus roseus* RLK1-like family of receptor-like kinases (Hématy et al. 2007; Engelsdorf et al. 2018). Perception of changes in pectin composition and activation of downstream responses are less characterized, though the FERONIA (FER) member of CrRLK1L family appears to be a possible sensor of pectin integrity (Feng et al. 2018; Lin et al. 2022). Turgor-sensitive processes appear to be relevant for the detection of CWI changes and the activation of downstream responses that restrict growth. For instance, several responses induced by isx are largely sensitive to osmotic manipulation by cotreatments with osmoticum (Hamann et al. 2009; Engelsdorf et al. 2018). Similarly, cell adhesion and elongation defects in *qua1* are suppressed by reducing external water potential via increased agar concentration in the growth medium (Verger et al. 2018).

Increasing evidence suggests that a feedback loop between auxin and cell wall composition regulates apical hook formation in Arabidopsis (Aryal et al. 2020; Baral et al. 2021; Jonsson et al. 2021). In particular, pectin composition seems to be associated to auxin response gradients and differential cell elongation during hook development (Jonsson et al. 2021). When auxin accumulates in the inner side of the hypocotyl, it promotes HG methylesterification, which correlates with a reduction in cell elongation (Jonsson et al. 2021). On the other hand, loss of asymmetric HG methylesterification in plants overexpressing a pectin methylesterase inhibitor alters the polar auxin transport machinery, disrupting the auxin gradient and resulting in a defective hook (Jonsson et al. 2021). In addition, alterations in other cell wall structural components, including cellulose (Sinclair et al. 2017; Baral et al. 2021) and xyloglucans (Aryal et al. 2020), also impair apical hook formation, suggesting that changes in various wall structural components converge into common responses that restrict differential cell elongation. However, the exact mechanisms linking CWI perception to the events that regulate hook development are not fully elucidated. Here, we report that loss of CWI represses a GA-modulated signaling module that comprises PIF4 and HLS1, resulting in a defective apical hook, and that these effects are suppressed by reduction of turgor pressure caused by low extracellular water potential. Our results suggest that turgor-dependent responses to altered CWI directly modulate signaling events that control differential cell expansion during hook formation.

Results

Defects in pectin biosynthesis impair hook formation and maintenance in a turgor-dependent manner

Apical hook formation was examined in a panel of Arabidopsis mutants impaired in different cell wall polysaccharides to determine the relative impact of changes in specific wall components on this process. Under our experimental conditions, 3 d after germination, etiolated wild-type (WT) seedlings displayed a completely closed hook (Fig. 1, A and B), which, in contrast, was completely open in *qua2-1* (henceforth, *qua2*) as well as in 2 other mutants affected in pectin composition, *gae1 gae6* and *murus1* (*mur1*; Fig. 1, A and B). The *gae1 gae6* double mutant carries mutations in 2 glucuronate 4-epimerases (GAEs) required for the biosynthesis of UDP-D-galacturonic acid (Mølhøj et al. 2004) and is defective in HG (like *qua2*) and, possibly, rhamnogalacturonan I (RG-I) biosynthesis (Bethke et al. 2016), while *mur1* is impaired in fucose biosynthesis (Bonin et al. 1997) and has therefore defective RG-II, xyloglucans, and cell wall glycoproteins (Reiter et al. 1993; Rayon et al. 1999; Freshour et al. 2003). In contrast, no significant difference in hook formation was observed in other cell wall mutants, namely *korrigan1* (*kor1*), impaired in primary cell wall cellulose deposition (Nicol et al. 1998), and *mur4* and *mur7* (Fig. 1, A and B), impaired in the biosynthesis of arabinose (Reiter et al. 1997; Burget et al. 2003), with the exception of *procuste1* (*prc1*; Desnos et al. 1996), that showed only a mild defect (Fig. 1, A and B). Taken together, these results suggest that mutations in genes involved in HG biosynthesis have a major impact on hook formation compared to genetic defects affecting other wall components.

Turgor pressure affects the activation of several responses triggered by loss of CWI (Hamann et al. 2009; Engelsdorf et al. 2018). To verify if turgor-dependent responses mediate the effects of altered pectin composition on hook formation and to determine what phases of this process are specifically affected, kinematic analysis was performed in WT, *qua2*, *gae1 gae6*, and *mur1* seedlings grown in the dark on medium containing 0.8% (w/v) or 2.5% (w/v) agar (henceforth indicated as low agar [LA] and high agar [HA], respectively). This method has been previously implemented to modulate turgor pressure in a controlled manner (Verger et al. 2018). WT seedlings grown on LA displayed typical hook development (Abbas et al. 2013), consisting in a formation phase, in which seedlings emerge from the seed and the hook angle reaches roughly 180° before 24 h after germination, followed by a maintenance phase, in which the hook is kept closed for about 48 h, and culminating in the opening phase, in which the hook opens reaching an angle of 0° (Fig. 2, A to C). In contrast, all mutants grown on LA showed a formation phase comparable, in length, to the WT, but were unable to form a fully closed hook (Fig. 2, A to C). Moreover, the maintenance phase was deeply compromised in all mutants, leading to hook opening right after the maximum curvature was achieved (Fig. 2, A to C).

When WT seedlings were grown on HA, formation and maintenance of the hook were largely unaffected, though the opening phase was accelerated (Fig. 2, A to C). Notably, growth on HA partially restored hook formation in all mutant lines (Fig. 2, A to C), leading to a significant increase in the maximum angle of curvature (Supplementary Fig. S1). In addition, HA also rescued the maintenance phase in *mur1* seedlings (Fig. 2B). Hook development could also be restored by sorbitol, an osmolyte previously shown

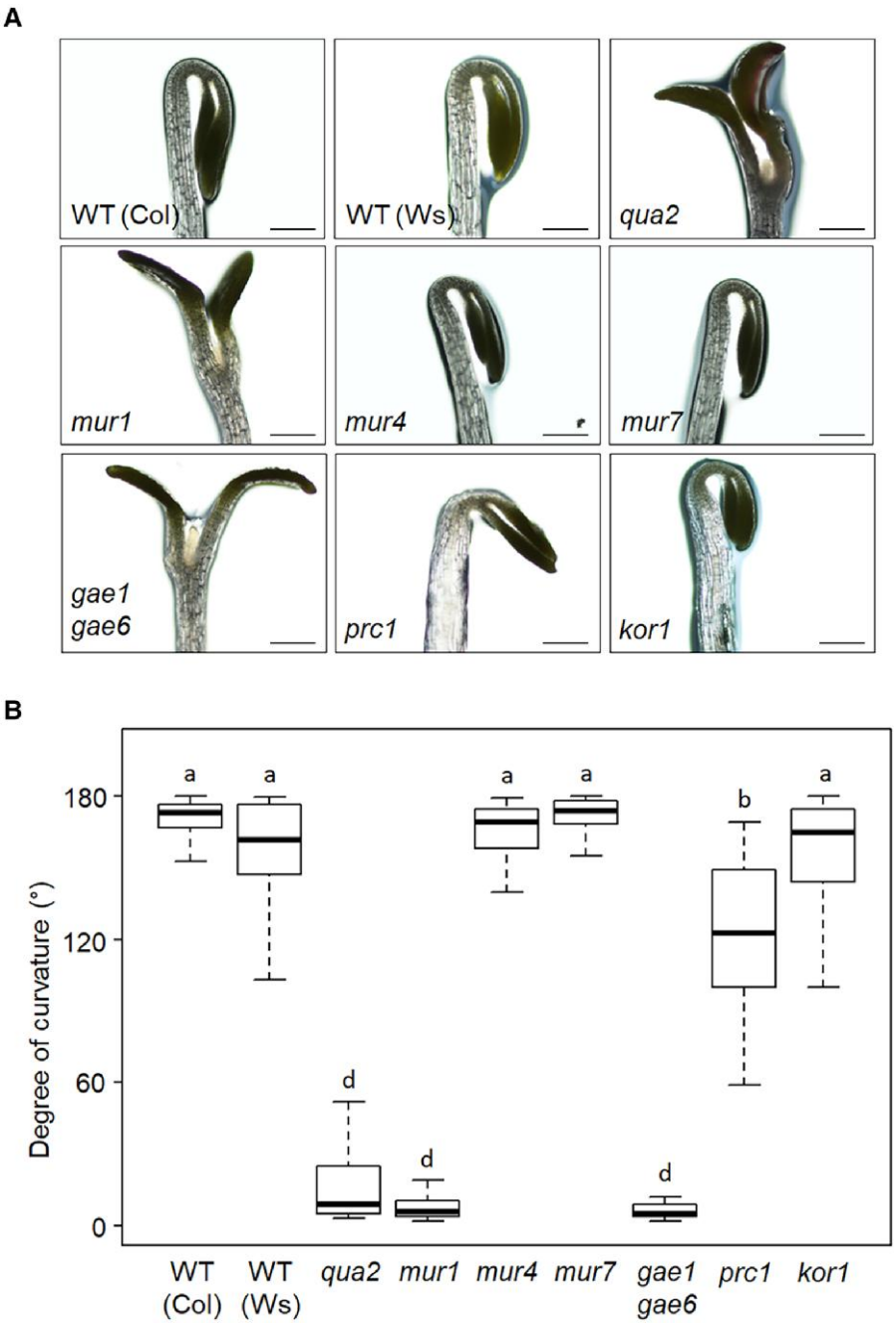

Figure 1. Apical hook formation in Arabidopsis cell wall mutants. **A)** Representative pictures of WT Col, WT Ws, *qua2*, *mur1*, *mur4*, *mur7*, *gae1 gae6*, *prc1* (in Col-0 background), and *kor1* (in Ws background) 3 d after germination. Scale bars in all panels, 0.5 mm. **B)** Quantification of apical hook angles of seedlings grown as in **A)**. Box plots indicate the 1st and 3rd quartiles split by median; whiskers show range ($n \geq 20$). Letters indicate statistically significant differences ($P < 0.05$) according to 1-way ANOVA followed by post hoc Tukey's HSD.

to suppress other responses induced by cell wall damage (Hamann et al. 2009; Engelsdorf et al. 2018; Supplementary Fig. S2). Taken together, these results indicate that the hook formation in seedlings with altered pectin composition is rescued under conditions that reduce turgor pressure.

Loss of pectin integrity disrupts differential cell expansion and asymmetric auxin response during apical hook development

Hook formation is thought to be largely dependent on the differential elongation rate of epidermal cell on the 2 sides of the hypocotyl (Silk and Erickson 1978). Defects in QUA2 restrict cell expansion in the epidermis of adult leaves (Raggi et al. 2015), suggesting that alterations in cell expansion rates might also occur in the epidermis of the hypocotyl of etiolated seedlings with altered pectin composition, resulting in a defective hook. Individual cell elongation rates were therefore measured in the apical portion of the hook of WT and, as illustrative of loss of pectin integrity, *qua2* seedlings grown in the dark in LA and HA conditions. As expected, cell expansion rate in WT seedlings was lower on the inner side than on the outer side of the hypocotyl, either in LA or HA condition (Fig. 3, A and B). In contrast, *qua2* seedlings showed a significant reduction in the expansion rate

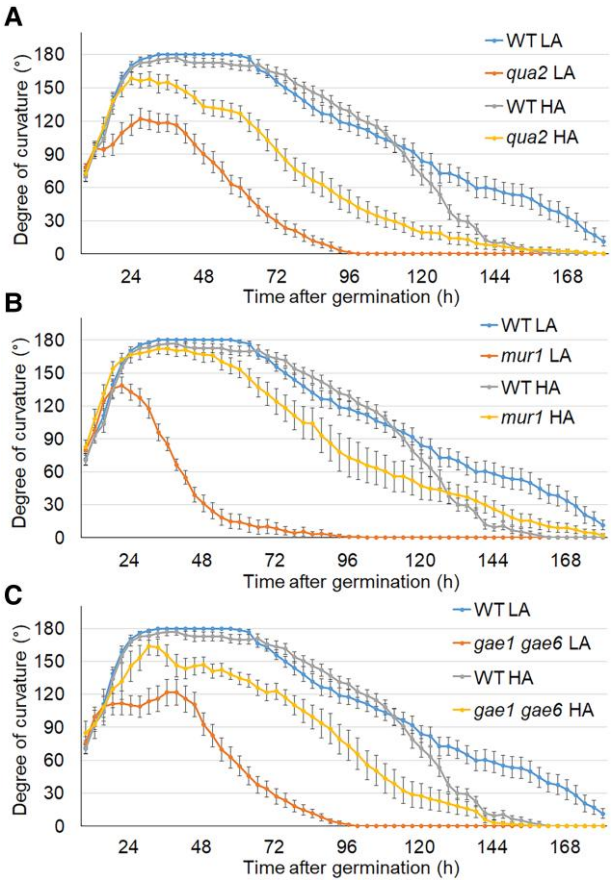

Figure 2. Kinematic analysis of apical hook formation in pectin mutants grown on LA and HA. WT and *qua2* **A)**, *mur1* **B)**, or *gae1 gae6* **C)** mutant seedlings were grown in the dark on medium containing either 0.8% (w/v) (LA) or 2.5% (w/v) agar (HA). The hook angle was measured at the indicated times. Error bars represent mean angle ± SE ($n \geq 15$).

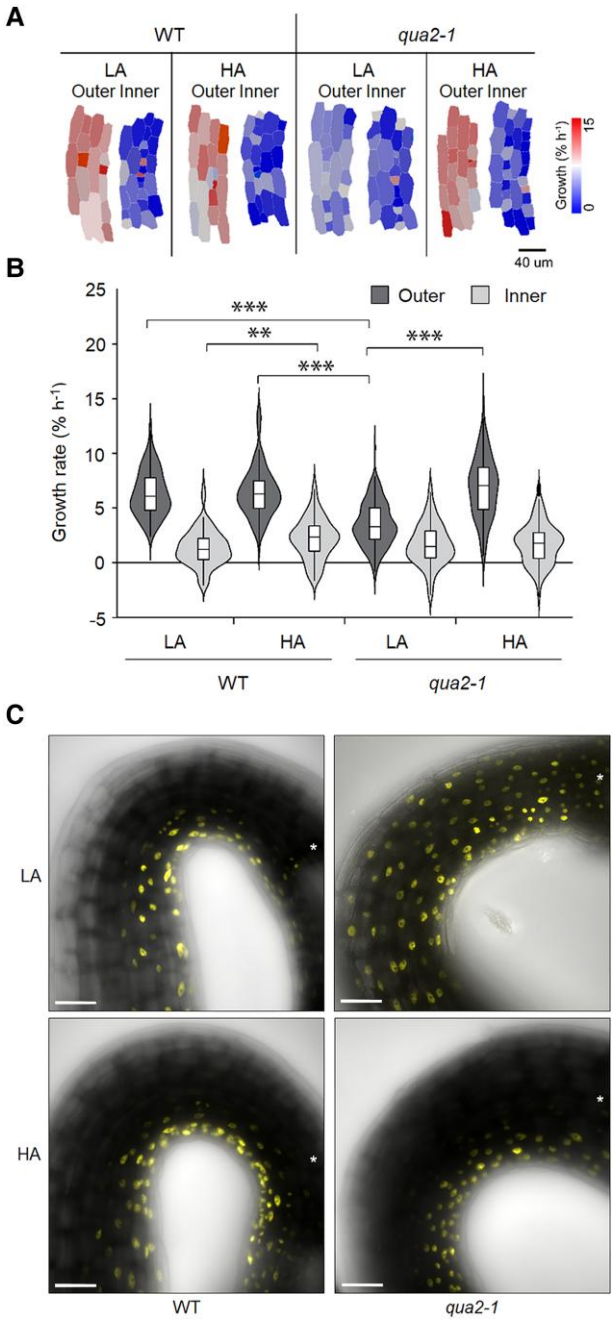

Figure 3. Effects of agar concentration on cell elongation and auxin response during apical hook formation in *qua2* seedlings. **A)** Heatmaps of the growth rate of individual cells in the apical portion of the hypocotyl upon a 3-h time lapse in WT and *qua2* seedlings grown in the dark on medium containing 0.8% (LA) or 2.5% (HA) (w/v) agar. **B)** Quantification of the growth rate of individual cells in the outer and inner sides of the hypocotyl of seedlings grown as in **A)**. Data are average of 3 independent biological replicates ± SD. In violin plots, the box limits represent the 1st and 3rd quartiles split by median, and whiskers show range. For each experiment, 15 cells from both the inner and outer sides of the hook were measured from each of 9 individual seedlings. Asterisks indicate statistical significance by Student's t test (**$P < 0.01$; ***$P < 0.001$). **C)** Representative confocal laser scanning microscopy images of WT and *qua2* seedlings expressing the DR5::Venus-NLS and grown in the dark on LA or HA. Asterisks in **C)** mark position of SAM. Scale bars in all panels, 50 μm.

in the outer side of the hook when grown on LA, but not on HA (Fig. 3, A and B).

As differential cell expansion is dependent on the establishment of an auxin gradient at the 2 sides of the apex (Abbas et al. 2013), the distribution of auxin response was evaluated in WT and *qua2* seedlings expressing the auxin response reporter *DR5*-VENUS-NLS (Heisler et al. 2005). WT seedlings displayed a strong fluorescent signal predominantly in the inner epidermal cells of the hook, and this pattern was not affected by the agar concentration in the medium (Fig. 3C). In contrast, reporter expression was equally distributed on both sides of the hypocotyl of *qua2* seedlings grown in LA (Fig. 3C). This alteration was fully restored when the mutant was grown on HA (Fig. 3C). Taken together, our results indicate that turgor-dependent responses to altered HG hinder proper asymmetric auxin signaling gradient and differential cell expansion during hook formation.

Loss of pectin integrity represses *HLS1* and *PIF4* expression and alters the expression of genes involved in GA homeostasis

HLS1 combines upstream stimuli important for hook formation (Guzmán and Ecker 1990), negatively regulating ARF2 levels (Li et al. 2004) and influencing auxin distribution (Lehman et al. 1996). Hook formation is also positively modulated by PIFs and, in particular, PIF4, which directly binds to the promoter of *HLS1* to activate its transcription (Zhang et al. 2018). We therefore evaluated if a defective pectin composition might affect the

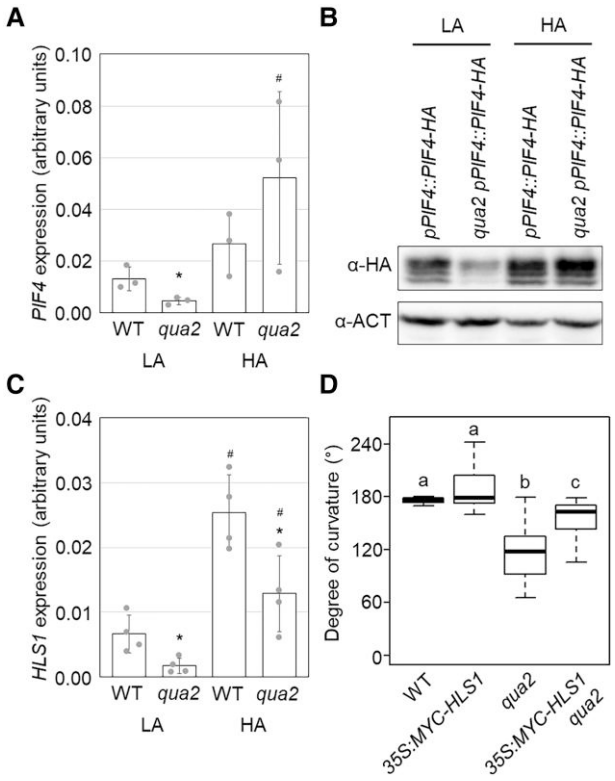

Figure 4. *HLS1* and *PIF4* expression in *qua2* mutant. Total RNA was extracted from WT and *qua2* seedlings 2 d after germination grown in the dark on medium containing 0.8% (LA) or 2.5% (HA) agar (w/v). **A)** Expression of *PIF4* was analyzed by RT-qPCR, using *UBQ5* as a reference. **B)** Transgenic lines expressing PIF4-HA under the control of its native promoter (ProPIF4:PIF4-3×HA) in *pif4*-101 or *qua2-1* background were grown on LA or HA medium. PIF4-HA levels were detected by immunoblot analysis with an antibody against HA; an antibody against actin (ACT) was used as a loading control. **C)** Expression of *HLS1* was analyzed by RT-qPCR, using *UBQ5* as a reference. Bars (in **A** and **C**) indicate mean of at least 3 independent biological replicates ± SD. Asterisks indicate statistically significant differences with WT according to Student's *t* test (*$P < 0.05$), and number signs indicate statistically significant differences with LA between same genotype according to Student's *t* test (#$P < 0.05$). **D)** Quantification of apical hook angles of WT, 35S:Myc-HLS1/*hls1-1*, *qua2*, and *qua2* 35S:Myc-HLS1/*hls1-1* seedlings 2 d after germination grown in the dark. Box plots in **D)** indicate the 1st and 3rd quartiles split by median; whiskers show range ($n \geq 20$). Letters indicate statistically significant differences ($P < 0.05$) according to 1-way ANOVA followed by post hoc Tukey's HSD.

expression of the genes encoding these proteins. In *qua2* seedlings grown under LA conditions, *PIF4* transcript levels were sharply reduced, compared to the WT, but increased to levels comparable to the WT under HA conditions (Fig. 4A). Consistently, *qua2* seedlings transformed with a HA-tagged version of PIF4 under the control of its native promoter (Zhang et al. 2017) displayed, under LA conditions, reduced levels of protein that strongly increased and reached levels comparable to the wild type when seedlings were grown in HA (Fig. 4B). Transcript levels of *HLS1* were also significantly reduced in etiolated *qua2* seedlings grown in LA, in comparison to the wild type, and significantly increased in both genotypes under HA conditions (Fig. 4C). These results suggest that reduced expression of *HLS1* might impair proper hook formation in *qua2*, and that its increased expression under HA conditions might restore it. Consistently, 2-d-old *qua2* seedlings expressing a myc-tagged version of HLS1 under the control of the constitutive CaMV 35S promoter (Shen et al. 2016) and grown under LA conditions displayed significantly greater hook angle than untransformed mutant seedlings (Fig. 4D).

Hook formation and *HLS1* expression are both positively regulated by GAs (An et al. 2012). We therefore evaluated if loss of pectin integrity might affect the expression of genes involved in the homeostasis of these hormones. Etiolated *qua2* seedlings grown on LA showed reduced transcript levels for *GA20ox1* and *GA3ox1*, required for GA biosynthesis (Hedden and Phillips 2000; Fig. 5, A and B), and increased expression of *GA2ox2*, involved in GA catabolism (Hedden and Phillips 2000; Fig. 5C). In contrast, under HA conditions, expression of these genes in WT and *qua2* seedlings was comparable (Fig. 5, A to C). Furthermore, exogenous GAs restored almost WT-like hook formation in *qua2* mutants grown on LA (Fig. 5D). Consistently, loss of all Arabidopsis *DELLA* genes (Feng et al. 2008) in the *qua2* background partially restored hook formation (Fig. 5E). Taken together, these results suggest that responses triggered by loss of pectin integrity, and dependent on turgor pressure, repress the GA-dependent PIF4-HLS1 signaling module, hindering proper hook formation.

isx inhibits hook formation and represses *HLS1* and *PIF4* expression and GA accumulation in a turgor-dependent manner

Our results indicate that defects in pectin composition caused by the *qua2* mutation induce responses dependent on turgor pressure that suppress GA-dependent signaling events important for hook formation. As *prc1*, impaired in the cellulose synthase CESA6 (Desnos et al. 1996), shows a partially defective hook (Fig. 1), we hypothesized that also defects in cellulose might have the same effects. To verify this hypothesis, a pharmacological approach was adopted, growing etiolated WT seedlings in the presence of isx, which targets cellulose synthases, including CESA6 (Desprez et al. 2002). Under LA conditions, at 2 d after germination, seedlings grown in the presence of isx at concentrations equal to or higher than 2.5 nM showed strongly reduced hook curvature (Fig. 6, A and B). HA conditions restored hook formation in the presence of isx at a dose of 2.5 nM and, to a lesser extent, 5.0 nM (Fig. 6, A and B). Analysis of WT seedlings expressing *DR5*-VENUS-NLS showed that, as observed in *qua2*, isx disrupted asymmetric auxin distribution in LA, but not in HA conditions (Fig. 6C). Consistently, in the presence of isx, cells on the outer side of the hook region of the hypocotyl showed a significant decrease in expansion rate, compared to control seedlings, only in LA, but not in HA conditions (Fig. 6, D and E). Overall, these data suggest that, as observed in *qua2*, also defects in cellulose deposition impair hook formation, disturbing the formation of an auxin asymmetric distribution and repressing cell elongation on the outer side of the hook.

Furthermore, as in *qua2*, isx repressed the expression of *HLS1* under LA, but not HA conditions (Fig. 7A). Notably, overexpression of a myc-tagged version of HLS1 in *hls1-1* seedlings (Shen et al. 2016) was sufficient to restore a fully closed hook in the presence of 2.5 nM isx (Fig. 7B). Treatments with isx also reduced *PIF4* transcript accumulation under LA, but not HA conditions (Fig. 7C). Consistently, isx repressed accumulation of PIF4 protein in a dose-dependent manner, but this effect was reduced under HA conditions (Fig. 7D). As observed in *qua2* seedlings, the expression of the biosynthetic *GA3ox1* and *GA20ox1* was repressed in plants treated with isx only in LA conditions, whereas expression in mock- and isx-treated seedlings was comparable in HA conditions (Supplementary Fig. S3, A to C). Moreover, exogenous GAs partially restored hook formation in seedlings treated with isx

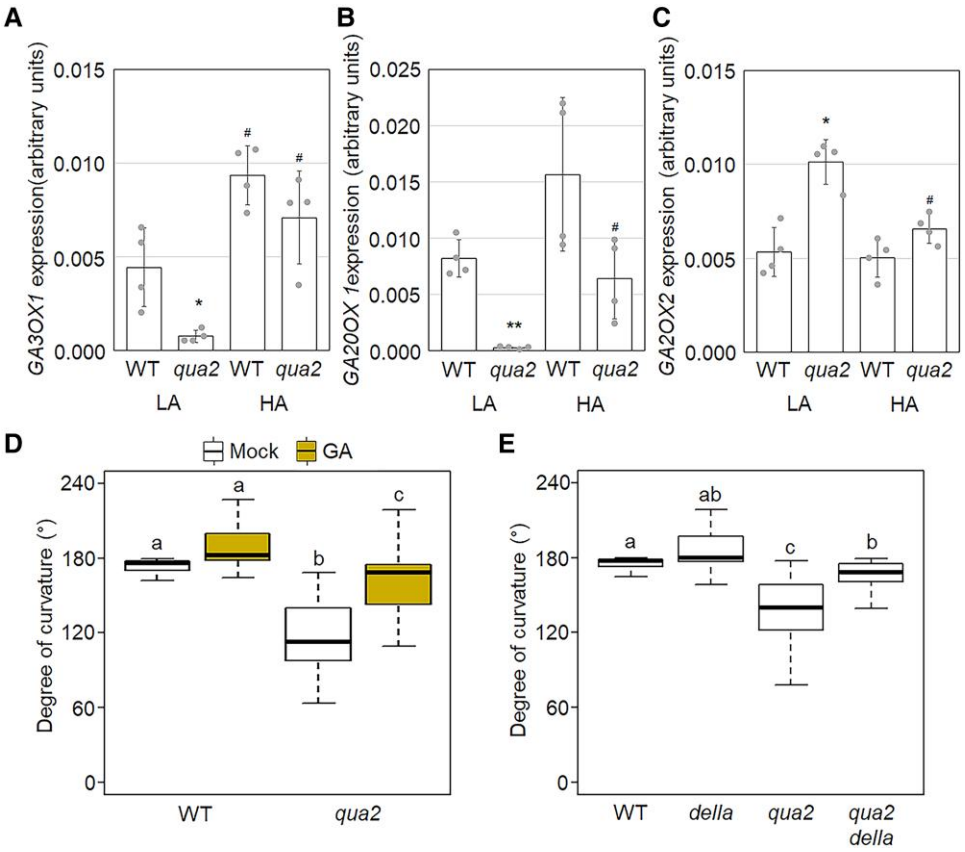

Figure 5. Defects in the expression of GA biosynthetic genes in *qua2* mutant. Expression of *GA3ox1* **A)**, *GA20ox1* **B)**, and *GA2ox2* **C)** in WT and *qua2* seedlings grown in LA and HA. Transcript levels were determined by RT-qPCR using *UBQ5* as a reference. Bars indicate mean of at least 3 independent biological replicates ± SD. Asterisks indicate statistically significant differences with WT according to Student's *t* test (*$P < 0.05$; **$P < 0.01$), and number signs indicate statistically significant differences with LA between same genotype according to Student's *t* test (#$P < 0.05$). **D)** Apical hook angles of WT and *qua2* seedlings 2 d after germination grown in the dark on medium supplemented with ethanol (mock) or 50 μM GA_4 (GA). **E)** Apical hook angles of WT Ler, *della*, *qua2*, and *qua2 della* sixtuple mutant seedlings 2 d after germination grown in the dark. Box plots in **D and E)** indicate the 1st and 3rd quartiles split by median; whiskers show range ($n \geq 20$). Letters indicate statistically significant differences, according to 2-way ANOVA followed by post hoc Tukey's HSD ($P < 0.05$).

(Fig. 8A). Hook formation in both the pentuple *della* mutant and in a *ga2ox* heptuple mutant, impaired in the GA catabolic GA2 oxidases GA2ox1/2/3/4/6/7/8 and therefore showing increased levels of active GAs in seedling hypocotyls (Griffiths et al. 2023), was less sensitive to isx (Fig. 8, B and C), suggesting that an alteration in GA homeostasis might contribute to the inhibition of hook formation in response to loss of CWI. To further investigate this hypothesis, we analyzed in vivo GA levels in response to isx using the Förster resonance energy transfer (FRET) biosensor Gibberellin Perception Sensor 2 (GPS2; Griffiths et al. 2023). Under LA conditions, GA levels in the hook region of the hypocotyl decreased in response to isx in a dose-dependent manner, while under HA conditions, GA levels appeared to be similar in control- and isx-treated seedlings (Fig. 8, D and E). These results indicate that, as in the case of *qua2*, isx downregulates GA-dependent signaling events that modulate *PIF4* and *HLS1* expression and control hook formation, suggesting a common mechanism underlying the effects of loss of CWI caused by alterations in different cell wall components on hook development.

As THE1 is a major player in the activation of responses triggered by altered cellulose deposition (Bacete and Hamann 2020), we evaluated if this protein is also important for the inhibition of apical hook formation mediated by isx. Indeed, hook curvature in 2 loss-of-function *the1-1* and *the1-6* mutants (Hématy et al. 2007; Merz et al. 2017) was less sensitive to isx both in LA and HA conditions (Fig. 9A). Conversely, the gain-of-function *the1-4* mutant (Merz et al. 2017) showed increased sensitivity to isx both in HA and LA media (Fig. 9A). Notably, both the *the1-1* and the *the1-6* mutations fully restored hook development in *qua2* seedlings (Fig. 9B). These results indicate that responses mediated by THE1 contribute to the defective hook development in plants with altered CWI.

Jasmonates are not involved in defective hook formation caused by altered CWI

isx induces the accumulation of jasmonates in Arabidopsis seedlings in a THE1-dependent manner (Engelsdorf et al. 2018). As exogenous jasmonic acid (JA) antagonizes apical hook formation in etiolated seedlings (Song et al. 2014; Zhang et al. 2014), we hypothesized that the hook defect observed in response to loss of CWI might be mediated by increased jasmonate levels. Levels of JA, jasmonyl-L-isoleucine (JA-Ile) and of the JA-derivative 11- and 12-hydroxyjasmonate (Σ 11-/12-OHJA, sum of unresolved 11- and 12-OHJA), were therefore quantified in dark-grown WT and *qua2* seedlings. Under LA conditions, mutant seedlings contained higher levels of all 3 jasmonates, compared to the wild type (Fig. 10A). Under HA conditions, the concentration of JA in WT seedlings was unaltered, while JA-Ile and Σ 11-/12-OHJA levels were moderately increased (Fig. 10A). Growth on HA medium

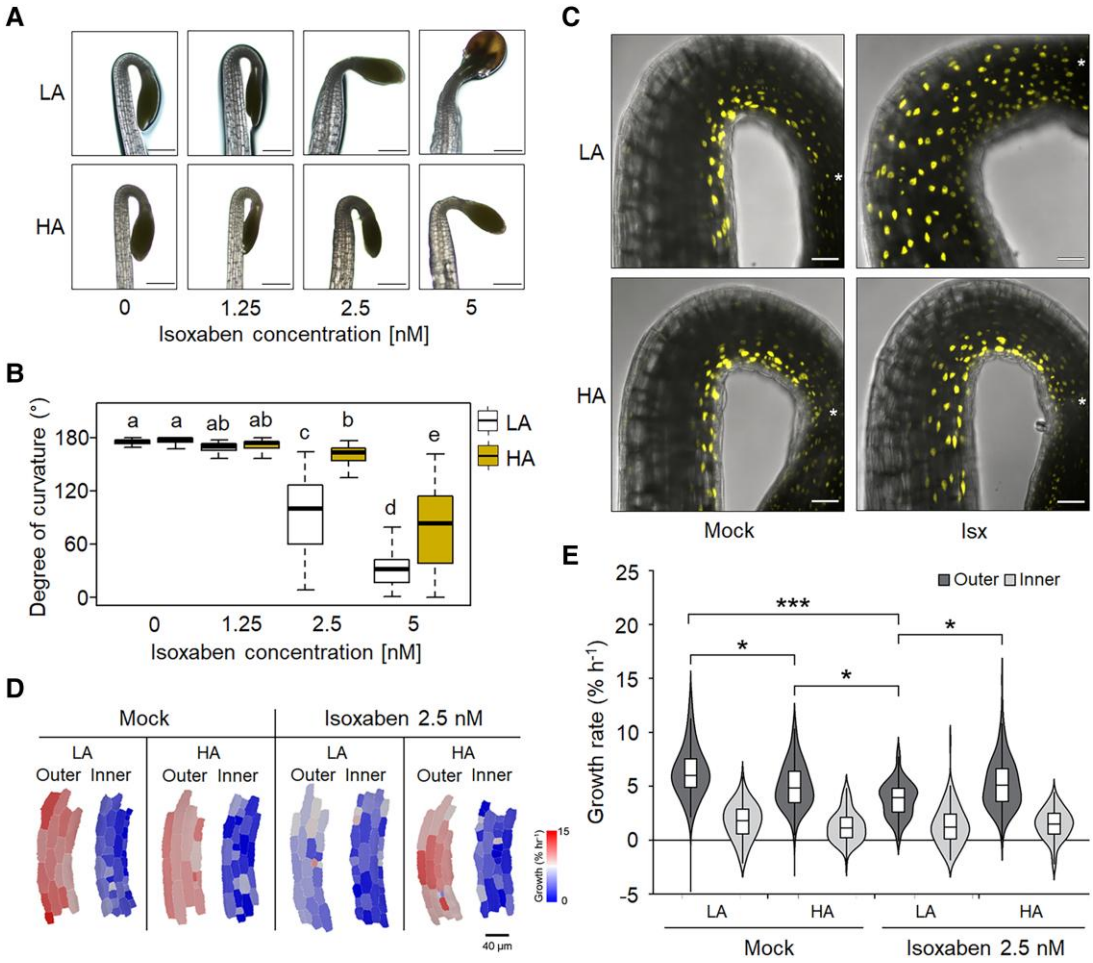

Figure 6. isx inhibits apical hook formation in a turgor-dependent manner. **A)** Representative pictures of WT seedlings 2 d after germination grown in the dark on medium 0.8% (LA) or 2.5% (HA) agar (w/v) and supplemented with isx at the indicated doses. Scale bars in all panels, 0.5 mm. **B)** Quantification of apical hook angles of WT seedlings grown as in **A)**. Box plots in **B)** indicate the 1st and 3rd quartiles split by median; whiskers show range ($n \geq 20$). Letters indicate statistically significant differences, according to 2-way ANOVA followed by post hoc Tukey's HSD ($P < 0.05$). **C)** Representative confocal laser scanning microscopy images of WT seedlings expressing the DR5::Venus-NLS grown in the dark with 2.5 nM isx in the dark on LA or HA. Asterisks in **C)** mark the position of SAM. Scale bars in all panels, 50 μm. **D)** Heatmaps of the growth rate of individual cells in the apical portion of the hypocotyl upon a 3-h time lapse in WT grown in the dark on medium containing 0.8% (LA) or 2.5% (HA) (w/v) agar supplemented with 2.5 nM isx. **E)** Quantification of the growth rate of individual cells in the outer and inner sides of the hypocotyl of seedlings grown as in **D)**. Data are average of 3 independent biological replicates ± SD. In violin plots, the box limits represent the 1st and 3rd quartiles split by median, and whiskers show range. For each experiment, 15 cells from both the inner and outer sides of the hook were measured from each of 9 individual seedlings. Asterisks indicate statistical significance by Student's *t* test (*$P < 0.05$; ***$P < 0.001$).

significantly reduced JA and JA-Ile levels in *qua2*, while Σ 11-/12-OHJA concentration in the mutant was slightly increased (Fig. 10A).

To assess whether high levels of jasmonates are responsible for the altered hook formation of *qua2*, this mutant was crossed with lines defective for *JASMONATE RESISTANT 1* (*JAR1*), required for the synthesis of JA-Ile (Wasternack and Hause 2013), or *CORONATINE INSENSITIVE 1* (*COI1*), a crucial component of the SCF COI1 E3 ubiquitin complex necessary for JA-Ile perception and transduction (Wasternack and Hause 2013). In *qua2 coi1* seedlings, 2 d after germination, hook impairment was slightly exacerbated (Fig. 10B), while the *qua2 jar1* double mutant did not show differences in hook angle, compared to *qua2* (Fig. 10C). Consistently, *jar1* and *coi1* single mutants treated with isx displayed hook defects comparable to those observed in the wild type (Fig. 10D). These results indicate that, despite loss of CWI triggers the accumulation of elevated levels of jasmonates in a turgor-dependent manner, these hormones do not contribute to the observed defects in hook formation.

Taken together, our results suggest that, in plants with altered CWI, turgor-dependent responses suppress, in a THE1-dependent manner, GA-mediated downstream signaling events controlling *PIF4* and *HLS1* expression. This leads to the disruption of auxin response asymmetry, differential cell elongation, and proper hook formation (Fig. 11).

Discussion

Cell wall alterations impair differential cell elongation during apical hook formation in a turgor-dependent manner

Differential cell elongation is widely used in plants to adapt growth and development to external and endogenous signals. This is exemplified by apical hook formation, which is largely dependent on the differential cell elongation on the opposite sides of the hypocotyl apex (Guzmán and Ecker 1990; Abbas et al. 2013). Cell elongation results from the interplay between turgor pressure and cell wall elasticity and extensibility (Ray et al. 1972). It is

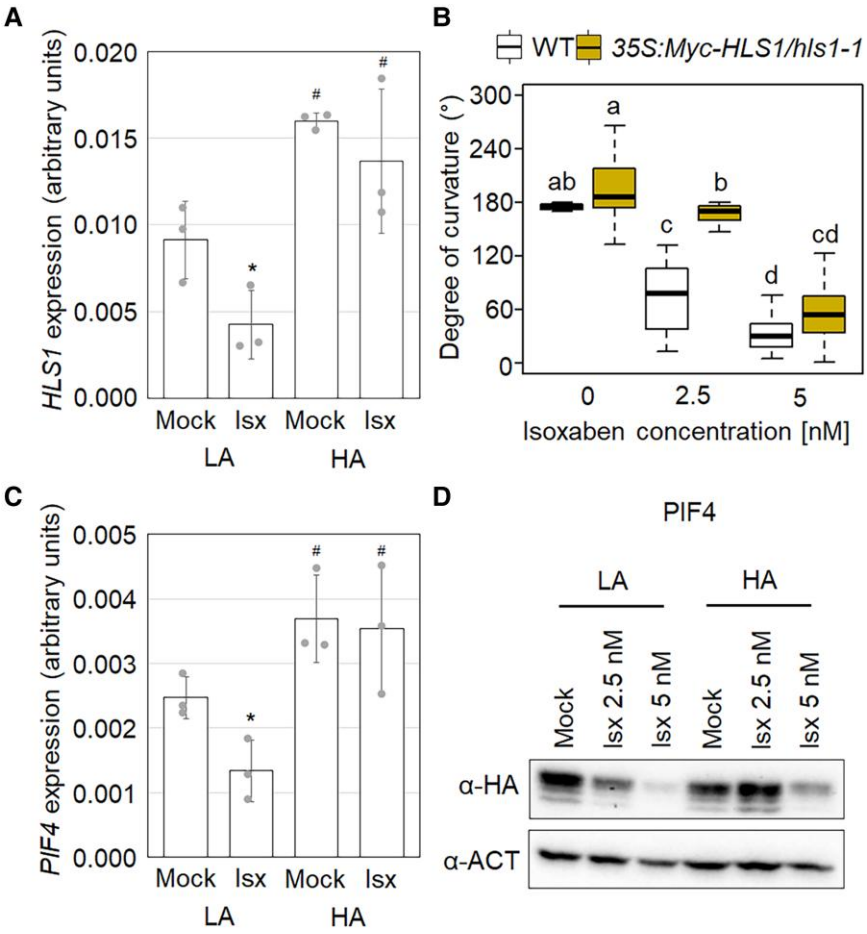

Figure 7. isx inhibits *PIF4* and *HLS1* expression in a turgor-dependent manner. **A)** Expression of *HLS1* in WT seedlings 2 d after germination grown in the dark with 2.5 nM isx in LA and HA. Transcript levels were determined by RT-qPCR using *UBQ5* as a reference. **B)** Quantification of apical hook angles of WT and 35S:Myc-HLS1/*hls1-1* seedlings 2 days after germination grown in the dark in the presence of the indicated concentrations of isx. **C)** Expression of *PIF4* in WT seedlings 2 d after germination grown in the dark with 2.5 nM isx in LA and HA. Transcript levels were determined by RT-qPCR using *UBQ5* as a reference. **D)** Transgenic lines expressing PIF4-HA under the control of its native promoter (ProPIF4:PIF4-3×HA) in *pif4*-101 background were grown on LA or HA medium supplemented with the indicated concentrations of isx. PIF4-HA levels were detected by immunoblot analysis with an antibody against HA; an antibody against actin (ACT) was used as a loading control. Bars in **A and C)** indicate mean of at least 3 independent biological replicates ± SD. Asterisks indicate statistically significant differences between mock- and isx-treated seedlings according to Student's *t* test (*$P < 0.05$); number signs indicate statistically significant differences between similarly treated seedlings grown on LA or HA according to Student's *t* test (#$P < 0.05$). Letters in **B)** indicate statistically significant differences according to 2-way ANOVA followed by post hoc Tukey's HSD ($P < 0.05$). Box plots indicate the 1st and 3rd quartiles split by median; whiskers show range ($n \geq 20$).

therefore not surprising that cell wall composition has a major impact on hook formation, and that an extensive interplay occurs between cell walls and the hormonal networks controlling hook formation (Aryal et al. 2020; Jonsson et al. 2021). However, despite our considerable knowledge of the signaling pathways controlling hook development, little is known of how cell walls interact with these pathways to modulate differential cell expansion and hook bending. Here, we have shown that changes in CWI, either caused by mutations in genes affecting pectin composition or by interference with cellulose deposition triggered by isx, hinder hook formation in Arabidopsis seedlings in a turgor-dependent manner. Moreover, altered CWI compromises, again in a turgor-dependent manner, asymmetric auxin maxima formation and differential cell elongation in the hook region. Additionally, turgor-mediated responses triggered by altered CWI downregulate hook-promoting signaling events that are positively regulated by GAs and include PIF4 accumulation and *HLS1* expression (Fig. 11). These results suggest that turgor pressure links CWI to GA-dependent signaling to modulate hook formation and maintenance.

Cell wall assembly and remodeling must be finely controlled during growth processes to ensure proper cell expansion while maintaining mechanical integrity (Wolf et al. 2012). Moreover, alterations in CWI can occur in response to abiotic or biotic stress (Vaahtera et al. 2019; Lorrai and Ferrari 2021); therefore, the structural and functional integrity of the wall must be constantly monitored and fine-tuned to allow normal growth and development under physiological conditions while preventing mechanical failure under adverse conditions (Rui and Dinneny 2020). Increasing evidence points to the role of turgor-mediated responses in triggering several effects of loss of CWI on plant growth and development (Engelsdorf et al. 2018; Verger et al. 2018). Indeed, plant cells must sustain huge turgor pressures, and their connection with each other, which is mediated by the cell wall, allows the propagation of signals generated by turgor pressure and by differential growth (Jonsson et al. 2022). Plants with altered CWI may fail to counterbalance turgor pressure, causing mechanical stress and triggering downstream compensatory responses. Indeed, supplementation with osmolytes, like sorbitol, or

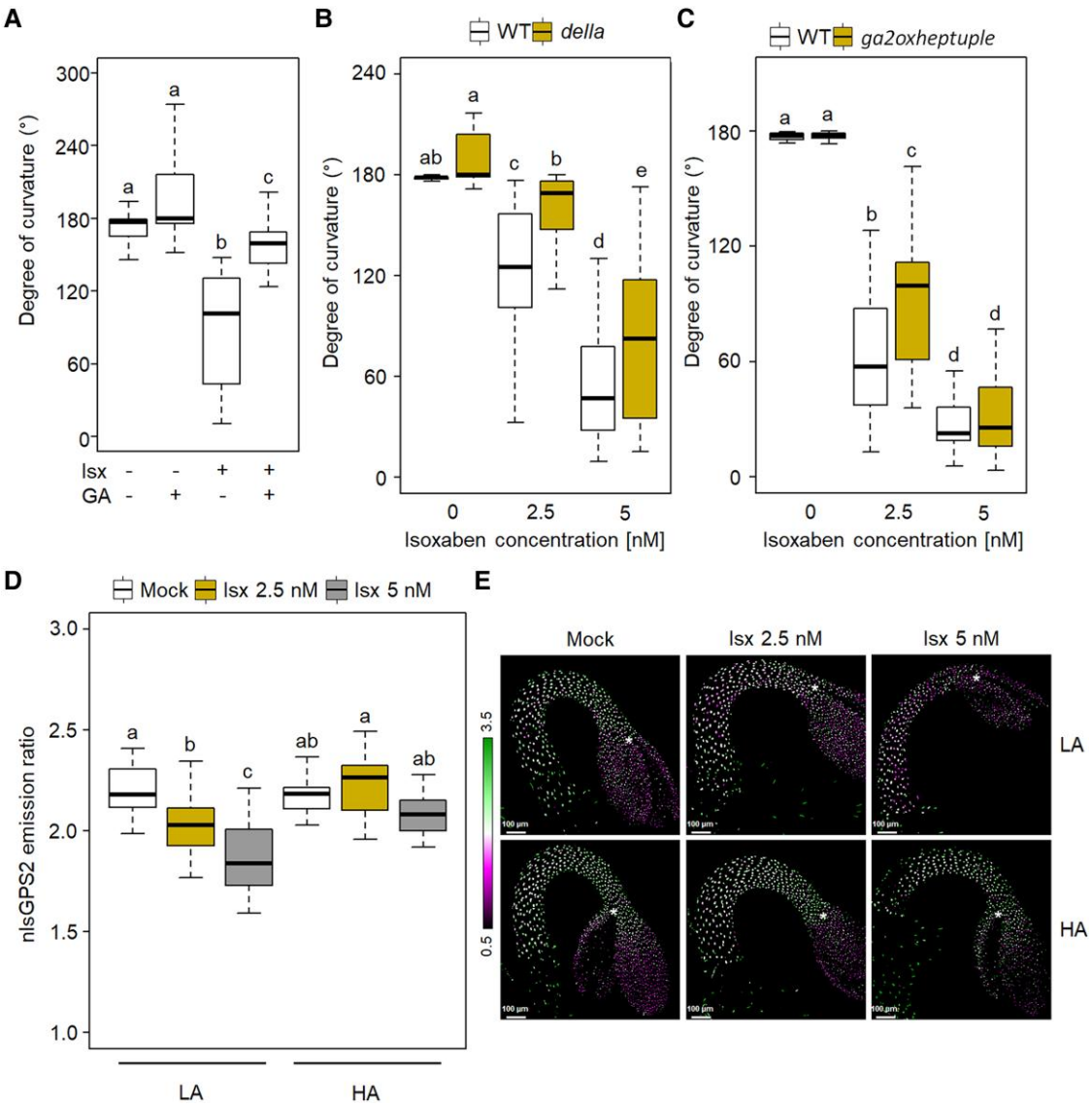

Figure 8. isx inhibits GA accumulation and signaling in a turgor-dependent manner. **A)** Apical hook angles of WT seedlings 2 d after germination grown in the dark and treated with DMSO or 2.5 nM isx in the presence or absence of 50 μM GAs. **B)** Apical hook angles of WT Ler and *della* seedlings 2 d after germination grown in the dark in the presence of isx at the indicated doses. **C)** Apical hook angles of WT Col-0 and *GA2oxheptuple* seedlings 2 d after germination grown in the dark in the presence of isx at the indicated doses. **D)** nlsGPS2 nuclear emission ratios from $n \geq 8$ hypocotyls of seedlings 1 d after germination grown in the dark in the presence of the indicated amount of isx on medium containing 0.8% (LA) or 2.5% (HA) agar (w/v). **E)** Representative images of nlsGPS2 emission ratios of the hypocotyls of seedlings grown as in **D)**. Letters in **A to D)** indicate statistically significant differences according to 2-way ANOVA followed by post hoc Tukey's HSD ($P < 0.05$). Box plots indicate the 1st and 3rd quartiles split by median; whiskers show range ($n \geq 20$) in **A to C)** ($n \geq 12$) in **D)**. Asterisks in **E)** mark position of SAM. Scale bars in all panels, 100 μm.

increasing medium agar concentrations have been previously exploited to decrease turgor pressure and restore growth in plants with perturbed cell walls (Engelsdorf et al. 2018; Verger et al. 2018; Bacete et al. 2022). We have found that both sorbitol and HA restore hook development in plants with altered pectin composition (Fig. 2; Supplementary Figs. S1 and S2). Analysis of cell growth rate showed that the impaired hook formation phase observed in *qua2* or in isx-treated seedlings is accompanied by a reduction of cell elongation rate in the outer cell layer and that WT-like growth rate was restored when seedlings were grown in HA condition (Figs. 3, A and B, and 6, D and E), further supporting the hypothesis that the compromised hook formation observed in plants with altered CWI is largely mediated by turgor-dependent mechanisms.

It has been proposed that loss of cell adhesion in plants with altered HG is a consequence of excessive tension in the epidermis caused by mechanical stress (Verger et al. 2018). Moreover, tension-mediated signals triggered by altered pectin composition might induce compensatory mechanisms that restrict cell expansion and therefore relieve mechanical stress. We have previously observed that the reduced cell expansion observed in *qua2* seedlings is at least partly mediated by an increased expression of *AtPRX71*, encoding a ROS-generating apoplastic peroxidase, which is also involved in H_2O_2 production in response to isx (Raggi et al. 2015). Notably, *AtPRX71* expression is also induced by hypoosmolarity (Rouet et al. 2006), a condition leading to excessive turgor pressure. This suggests that turgor-dependent responses triggered by altered CWI might lead to compensatory mechanisms, possibly

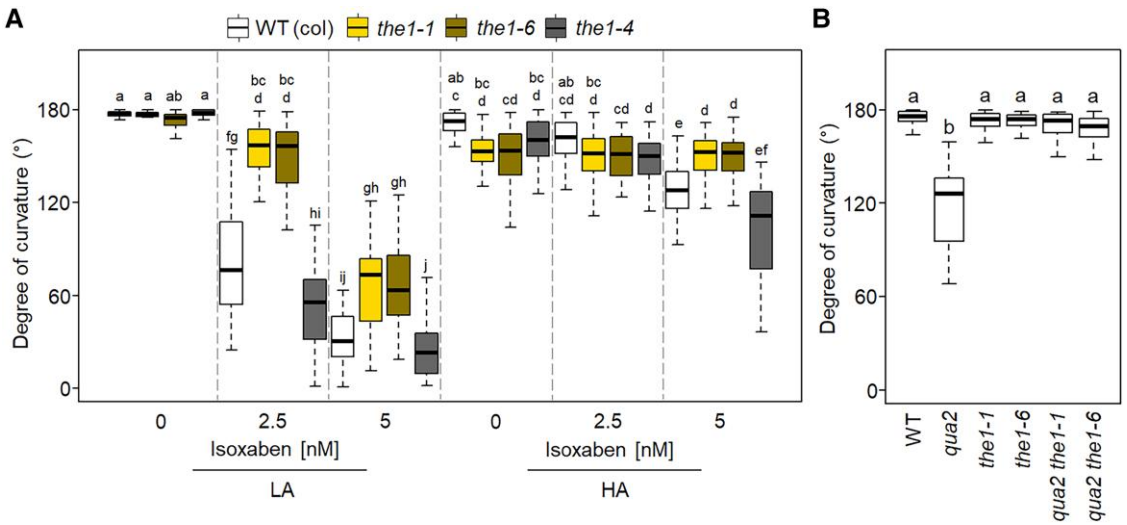

Figure 9. Apical hook inhibitions by isx supplementation or *qua2* mutation is dependent on THE1. **A)** Quantification of apical hook angles of WT (Col-0), *the1-1*, *the1-6*, and *the1-4* seedlings 2 d after germination grown in the dark on medium 0.8% (LA) or 2.5% (HA) agar (w/v) and supplemented with isx at the indicated doses. **B)** Quantification of apical hook angles of WT, *qua2*, *the1-1*, *the1-6*, *qua2 the1-1*, and *qua2 the1-6* seedlings 2 d after germination grown in the dark. Letters indicate statistically significant differences according to 2-way ANOVA followed by post hoc Tukey's HSD ($P < 0.05$). Box plots indicate the 1st and 3rd quartiles split by median; whiskers show range ($n \geq 20$).

including peroxidase-mediated cell wall crosslinking, that ultimately restrict cell expansion. Such mechanisms might take place also during apical hook formation, causing the turgor-dependent defect in differential cell expansion observed in *qua2* and in isx-treated seedlings.

The observation that both the *qua2* mutation and isx impair proper hook formation under LA but not HA conditions indicates that loss of CWI caused by alterations in either HG or cellulose trigger turgor-dependent signals that hinder differential cell expansion. However, the exact nature of these signals still needs to be clarified. It has been proposed that loss of CWI results in distortion or displacement of the plasma membrane relative to the cell wall that can be detected by a dedicated CWI maintenance mechanism (Engelsdorf et al. 2018). Our results suggest that THE1 plays an important role in mediating pectin- and isx-triggered inhibition of hook formation, possibly controlling the activation of responses that lead to reduced cell expansion. It has been recently proposed that THE1 might indirectly influence changes in cell wall stiffness in response to ISX/sorbitol cotreatments, possibly as a consequence of THE1 function in modulating responses to ISX (Bacete et al. 2022). Further investigation will provide insights into the role of specific components of the CWI maintenance system in modulating differential cell expansion during hook formation.

Loss of CWI represses a signaling module that promotes apical hook development

Differential elongation during hook development requires the formation of an auxin gradient, reaching a maximum on the inner side of the hook where it reduces the cell growth rate (Abbas et al. 2013). The cell wall is a key hub in this process, as a positive feedback loop mechanism couples cell wall stiffness, mediated by changes in the degree of methylesterification of HG, with auxin redistribution (Jonsson et al. 2021). However, the mechanisms linking changes in cell wall properties and the signaling pathways that modulate differential cell expansion are poorly understood. Our results suggest that loss of CWI represses a signaling module, comprising PIF4 and HLS1, that positively regulates auxin biosynthesis and distribution and ultimately hook formation (Lehman et al. 1996; Franklin et al. 2011; Zhang et al. 2018). HLS1 suppresses the accumulation of ARF2 (Li et al. 2004), which negatively regulates hook formation and transcriptional control of auxin transporters downstream of xyloglucan defects (Aryal et al. 2020). We observed that mutants with altered pectin composition and seedlings treated with isx show a reduction of *HLS1* and *PIF* transcript levels (Figs. 4, A and C, and 7, A and C) and of PIF4 protein levels (Figs. 4B and 7D). The downregulation of *HLS1* and *PIF4* might contribute to the disruption of asymmetric auxin maxima and differential cell expansion observed in *qua2* and might also contribute to the hook defect caused by altered cellulose deposition, as HLS1 overexpression confers partial resistance to the inhibitory effect of isx (Fig. 7B) and of *qua2* mutation (Fig. 4D). These observations point to a common regulation of hook formation in response to changes in different cell wall components.

Mechanical stress arising from turgor pressure changes can activate JA-mediated stress responses in plants with altered CWI (Engelsdorf et al. 2018). Recently, it has been proposed that JA-Ile accumulation in the roots of the *kor1* mutant is prompted by turgor-driven mechanical compression at the level of the cortex (Mielke et al. 2021). We found that *qua2* seedlings accumulate high levels of jasmonates, which decrease when the mutant is grown in HA conditions (Fig. 10A), confirming that cell wall stress-induced JA production is mediated by turgor pressure changes. However, JA signaling does not appear to be involved in the repression of hook development caused by loss of CWI neither in *qua2* nor in isx-treated seedlings (Fig. 10, B to D). On the other hand, our results suggest that hook defects in plants with an altered cell wall might be at least partially mediated by a reduction in GA accumulation, as (i) GA levels are reduced in isx-treated seedlings (Fig. 8, D and E) under LA conditions and are restored by HA; (ii) both *qua2* and isx-treated WT seedlings show altered expression of genes involved in the homeostasis of GAs (Fig. 5, A to C; Supplementary Fig. S3); (iii) exogenous GAs restore hook formation in *qua2* and in isx-treated WT seedlings (Figs. 5D and 8A); and (iv) lack of DELLA or GA2ox proteins that increase GA response

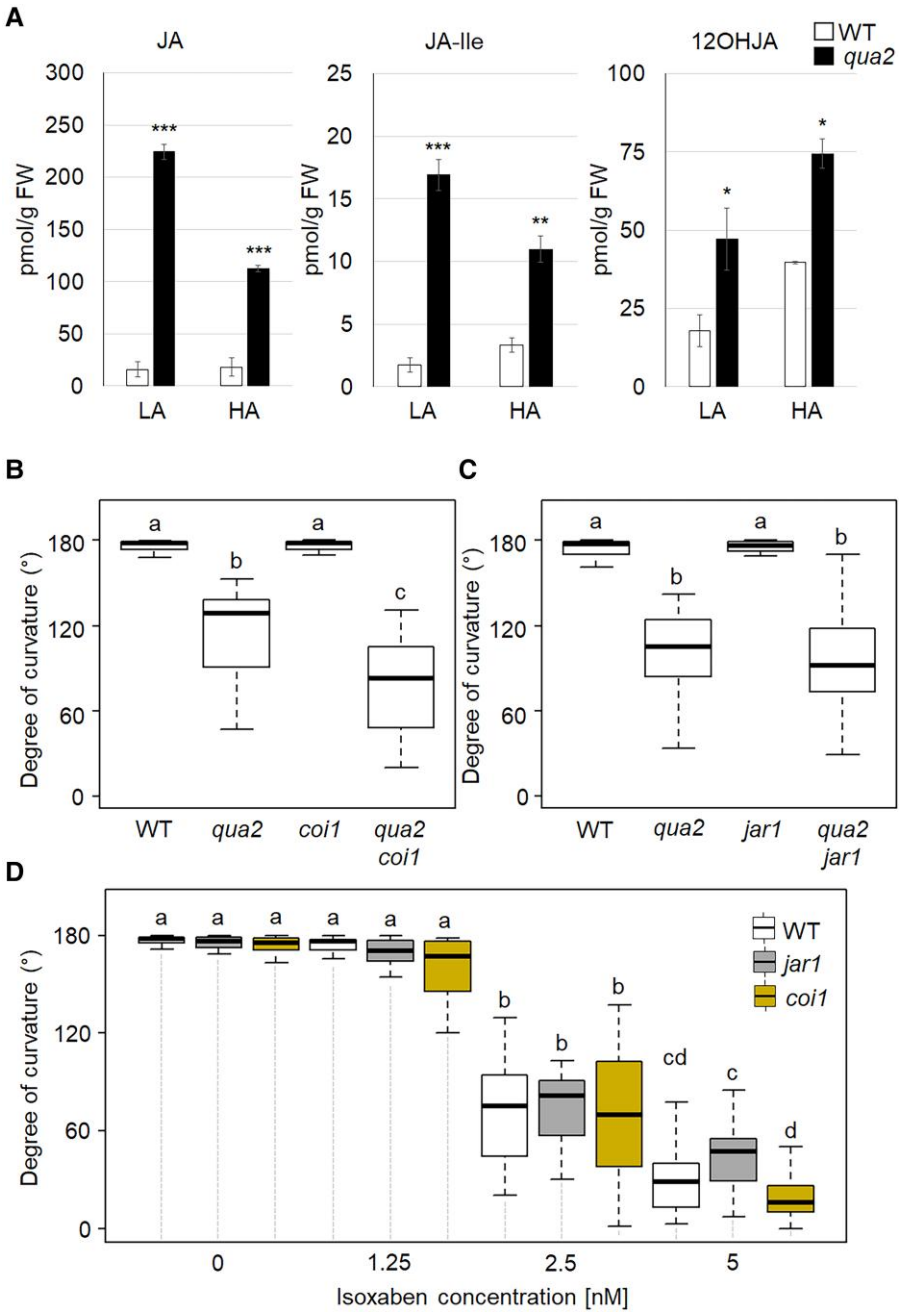

Figure 10. Inhibition of apical hook formation in response to altered CWI is independent of jasmonate signaling. **A)** Levels of JA, JA-Ile, and Σ 11-/12-OHJA in WT and *qua2* seedlings 2 d after germination grown in the dark on medium containing 0.8% (LA) or 2.5% (HA) agar (w/v). Bars represent means of 3 independent biological replicates ± SD. Asterisks indicate significant differences relative to WT, according to Student's *t* test (*$P \leq 0.05$; **$P \leq 0.01$; ***$P \leq 0.001$). **B and C)** Apical hook angles of WT, *qua2*, *coi1*, and *qua2 coi1* **B)** or *jar1* and *qua2 jar1* **C)** grown as in **A)**. **D)** Quantification of apical hook angles of WT (WT Columbia), *jar1*, and *coi1* seedlings 2 d after germination grown in the dark in the presence of isx at the indicated doses. Box plots in **B to D)** indicate the 1st and 3rd quartiles split by median, and whiskers show range ($n \geq 20$). Letters indicate statistically significant differences ($P < 0.05$) according to 2-way ANOVA followed by post hoc Tukey's HSD.

or levels, respectively, reduces the impact of isx on hook formation (Fig. 8, B and C). Notably, growth of seedlings on HA increases *HLS1*, *PIF4*, and GA biosynthetic gene expression in both *qua2* and isx-treated seedlings (Figs. 4, A and C, 5, A to C, and 7, A and C; Supplementary Fig. S3), and overexpression of HLS1 restores hook formation in *qua2* and in isx-treated seedlings (Figs. 4D and 7B). Furthermore, HA conditions prevent the reduction of PIF4 protein levels in *qua2* and in isx-treated seedlings (Figs. 4B and 7D). These results suggest a causal link between altered CWI, reduction of GA levels, and suppression of GA-mediated signaling required for proper auxin signaling and differential cell expansion during hook formation and maintenance.

In conclusion, our results indicate that turgor-dependent responses link changes in CWI to the downregulation of a regulatory module, comprising GAs, PIF4 (and, possibly, other PIFs), and HLS1, that promotes asymmetric cell elongation and hypocotyl curvature during hook formation (Fig. 11). However, it cannot be ruled out that additional mechanisms might contribute to compromise hook formation in plants with defective cell wall composition. Intriguingly, it was reported that short fragments

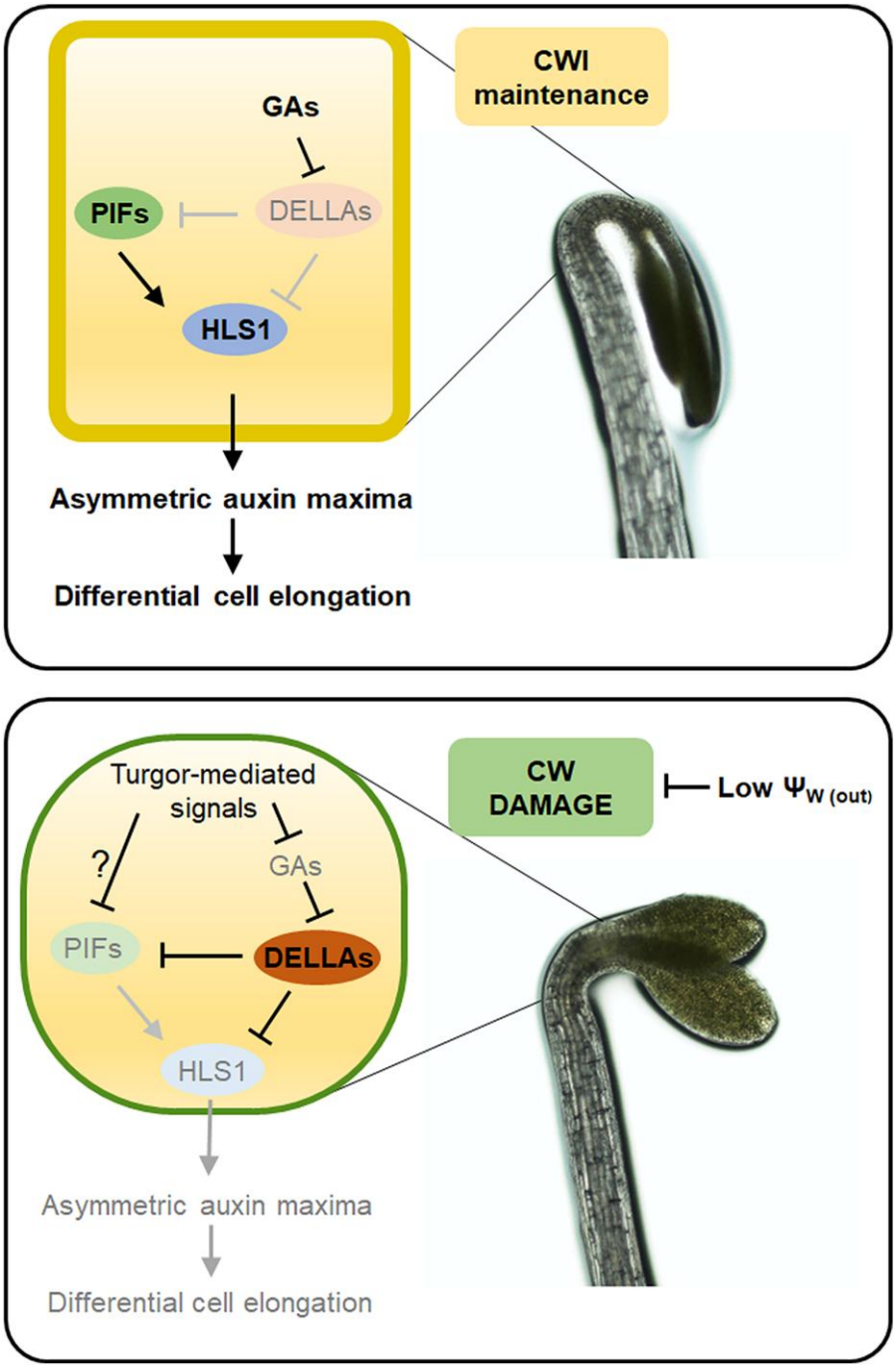

Figure 11. Proposed model of the effects of loss of CWI on apical hook formation. Perturbation of CWI, either caused by mutations in pectin composition or by isx, activates turgor-dependent responses that repress accumulation of active GAs, leading to stabilization of DELLA proteins and reduction of PIF4 and possibly other PIF protein levels. Increased DELLAs and reduced PIFs result in impaired *HLS1* expression, impairing proper formation of auxin response maxima and differential cell elongation and ultimately inhibiting apical hook development. The arrows indicate positive regulation, and blunt-ended bars indicate inhibition. Question mark indicates unidentified signaling elements. Elements in gray indicate reduction of levels or reduced downstream responses. Ψ_w, water potential; PIFs, PHYTOCHROME INTERACTING FACTORs; HLS1, HOOKLESS1; DELLAs, DELLA proteins; GAs, gibberellins; CW, cell wall; CWI, cell wall integrity.

of HG restore hook development in dark-grown mutants impaired in pectin composition (Sinclair et al. 2017), suggesting that, in WT plants, HG-derived fragments might act as signals that promote hook formation. Future research will help elucidate the mechanisms linking changes in the cell wall biochemical and physical properties occurring in response to internal and environmental cues to the signaling cascades that modulate differential cell growth during plant developmental programs.

Materials and methods

Plant lines

All experiments were performed using Arabidopsis (*A. thaliana*) lines. The *qua2-1* mutant was a kind gift of Gregory Mouille (INRA Centre de Versailles-Grignon); *coi1-1* and *jar1-1* mutants were a gift of Edward Farmer (Department of Plant Molecular Biology, University of Lausanne). The *mur1-1*, *mur4-1*, *mur7-1*,

prc1-1, *kor1-1*, and *gae1-1 gea6-1* mutants and the pentuple *della* mutant (*gai-t6*, *rga-t2*, *rgl1-1*, *rgl2-1*, and *rgl3-1*) were obtained by the Nottingham Arabidopsis Stock Centre. The transgenic *PIF4p:PIF4-HA pif4-301* (Zhang et al. 2017) line was a kind gift of Christian Fankhauser (University of Lausanne, Center for Integrative Genomics). The 35S::Myc-HLS1/*hls1-1* line was a gift by Shangwei Zhong (Peking University). The *the1-1*, *the1-4*, and *the1-6* mutants were a gift by Herman Höfte (INRA Centre de Versailles-Grignon). Generation of the *ga2oxheptuple* mutant (*ga2ox1/2/3/4/6/7/8*) is described in Griffiths et al. (2023).

The *qua2-1 coi1-1* and *qua2-1 jar1-1* double mutant lines were generated by crossing single mutants. Double homozygous lines were isolated based on the presence of cell adhesion defects in the hypocotyl and on primary root resistance to exogenous JA. *qua2-1 coi1-1* double homozygous mutants were crossed with a *qua2-1/qua2-1 coi1-1/COI1* sesquimutant, and homozygous individuals of the segregating progeny were selected based on their insensitivity to JA in terms of root elongation. The *qua2-1 the1-1* and *qua2-1 the1-6* double mutant lines were generated by crossing single mutants. Double mutants were screened for *qua2-1* homozygous mutation for the presence of cell adhesion defects in the hypocotyl, while PCR was used to identify *the1-1* and *the1-6* homozygous individuals. The *qua2-1* 35S::Myc-HLS1/*hls1-1*, *qua2-1* homozygous mutation was identified by the presence of cell adhesion defects while 35S::Myc-HLS1/*hls1-1* was isolated by PCR.

The *PIF4p:PIF4-HA pif4-301 qua2-1* line was generated by crossing. The *qua2* DR5-VENUS line was generated by crossing a WT line expressing DR5-VENUS (*pDR5rev::3XVENUS-N7*; Heisler et al. 2005) with *qua2-1*. The *qua2-1* myr-YFP line, expressing the myr-YFP plasma membrane marker line, was obtained by crossing a WT line carrying the pUBQ10::myr:YFP construct (Willis et al. 2016) with a homozygous *qua2-1* line. In all cases, double *qua2-1* homozygous individuals were isolated based on the presence of cell adhesion defects in the hypocotyl, and homozygosity of the transgene was confirmed based on the F3 generation.

All lines used in this work were in the Col-0 background, except for *kor1-1*, in Wassilewskija (Ws) background, and *della*, in Landsberg erecta (Ler) background.

Plant growth conditions

Seeds were surface sterilized with absolute ethanol (v/v), air dried, and sown on a solid medium containing 2.2 g/L MS salts (Duchefa), 1% (w/v) Suc, and 0.8% or 2.5% (w/v) plant agar (Duchefa), pH 5.6. Plates were wrapped in aluminum foil and stratified at +4 °C for 2 to 3 d. isx (Merck) was dissolved in 0.01% (v/v) DMSO and supplemented to a growth medium at indicated concentrations. For etiolated growth, after stratification, germination was induced by exposure to white light for 4 to 6 h, and plates were wrapped in aluminum foils and placed in a growth chamber for the indicated days. Images of the apical hook were acquired with an optical microscope using 5× magnification with light from below the sample at the indicated time after germination. For hook angle analysis with sorbitol supplementation, seeds were sown on a sterilized nylon mesh placed on agar medium plates without sorbitol and placed in the dark as described above. After 24 h, the nylon mesh was transferred under a green dim light to new plates containing sorbitol. All supplements were added in the indicated concentrations to autoclaved control media. For RNA and protein analysis, seedlings were harvested under dim green light and flash frozen in liquid nitrogen.

Kinematic analysis of apical hook development and cell elongation measurement

Seedlings were grown vertically on solid medium plates in the dark at 21 °C, illuminated with far infrared light (940 nm). Seedlings were photographed every hour using a Raspberry Pi camera (www.raspberrypi.com). Apical hook angles were measured using ImageJ software (http://imagej.nih.gov/ij/).

For time-lapse imaging of cell expansion, WT myr-YFP and *qua2-1* myr-YFP seedlings were imaged using a Zeiss LSM800 confocal microscope equipped with 10×/0.45 Plan-apo dry objective. Z-stacks were acquired without averaging with a 0. 62-micron cubic voxel size. YFP excitation was performed at 525 nm wavelength (laser intensity between 1% and 3.2%), and the emission was collected at 400 to 650 nm for (donor emission), gain between 620 and 650. Dark-grown seedlings were placed on an agar gel block on a microscopy slide and imaged at 3-h intervals. Between the acquisition of images, seedlings were placed vertically in a dark chamber to maintain skotomorphogenic conditions. Cell elongation was calculated using the software MorphographX (MGX). Using MGX, epidermal cell surface area from Z-stacks was extracted as described previously (Barbier de Reuille et al. 2015). The longitudinal expansion was calculated in MGX by overlaying Z-stacks with a fitted curved Bezier grid providing axial growth coordinates. For each condition and genotype, 15 cells from both the inner and the outer sides of the hook were measured from each of 9 individual seedlings (135 cells). The data were statistically analyzed by 2-tailed Student's *t* test.

Gene expression analysis

To analyze gene expression, the uppermost part of seedling hypocotyls, including the apical hook, was isolated using a razor blade, frozen in liquid nitrogen, and homogenized with an MM301 ball mill (Retsch, Germany) mixer ill for about 1 min at 25 Hz. Total RNA was extracted with NucleoZOL reagent (Macherey-Nagel, Germany) according to the manufacturer's instructions. One microgram of total RNA was retrotranscribed with ImProm II Reverse Transcriptase (Promega, USA). cDNA was mixed with iTaq Universal SYBR Green Supermix (Bio-Rad) and amplified using a CFX96 Real-time System (Bio-Rad, USA) using primer pairs specific for the genes of interest (Supplementary Table S1). Expression levels of each gene, relative to the *UBIQUITIN5* (*UBQ5*), were determined using a modification of the Pfaffl method (Pfaffl 2001) as previously described (Ferrari et al. 2006).

Protein extraction and immunoblot assays

Total proteins were extracted from etiolated seedlings ($n = 30$) grounded in liquid nitrogen and resuspended in 120 μL of extraction buffer (125 mM Tris, pH 6.8, 4% [w/v] SDS, 20% [v/v] glycerol, 0.02% [w/v] bromophenol blue, and 10% [v/v] β-mercaptoethanol). Samples were heated for 5 min at 95 °C and centrifuged for 1 min at 15,000 × *g* at room temperature. Proteins (20 μL of each sample) were separated by 8% (v/v) acrylamide SDS-PAGE and transferred to a nitrocellulose membrane using the Trans-Blot Turbo transfer kit (Bio-Rad, USA). Five percent (w/v) milk dissolved in phosphate-buffered saline with 0.05% (v/v) Tween 20 (Sigma) was used for blocking for 1.5 h at room temperature and antibody dilutions. For the detection of HA, a 1:1,000 dilution of the (F-7) sc-7392 antibody (Santa Cruz Biotechnology, USA) was used. As a secondary antibody, a 1:2,000 dilution of horseradish peroxidase (HRP)-conjugated anti-mouse immunoglobulin (Cell Signaling Technology, USA) was used. An anti-actin polyclonal primary antibody (Agrisera) was used as a loading

control, with HRP-conjugated anti-rabbit immunoglobulin (1:2,000; Cell Signaling) as a secondary antibody. The chemiluminescent signal of HRP conjugated to secondary antibodies was detected with ECL Western Blotting Substrate (Promega, USA) using a ChemiDoc XRS+ system (Bio-Rad, USA).

Confocal laser scanning microscopy

For DR5::VENUS detection, 2 d after germination, etiolated seedlings were placed between a microscopy slide and a cover slip. Images were acquired using a Zeiss LSM 880 laser scanning confocal microscope, using the Zen black software, with a 20× (C-Apochromat 20×/1.2 W Korr FCS M27) objective. Z-stacks were acquired without averaging with the image size 1,024 × 1,024 pixels and 0.345-micron pixel size and a Z-step size of 1 μm. VENUS excitation was performed at 514 nm wavelength (laser intensity 1%), and the emission was collected in the 518 to 560 nm range, gain 600. The laser reflection was filtered by a beam splitter.

For in vivo GA analysis, 1 d after germination, dark-grown seedlings were mounted in liquid 1/4× MS medium (1/4× MS salts, 0.025% [w/v] MES, pH5.7), covered with a coverslip, and the entire hypocotyl was imaged. Confocal images were acquired with a format of 1,024 × 1,024 pixels and a resolution of 12 bit on an upright Leica SP8-iPhox using a 20× dry objective. For FRET analysis, the same settings described in Rizza et al. (2017) were applied. The 3 fluorescence channels collected for FRET imaging were as follows: Cerulean donor excitation and emission or DxDm, Cerulean (CFP) donor excitation, Aphrodite (YFP) acceptor emission or DxAm, and Aphrodite acceptor excitation and emission or AxAm. CFP excitation was performed at 448 nm wavelength (laser intensity 5%), and the emission was collected at 460 to 500 nm for CFP (donor emission) and 525 to 560 nm for YFP (FRET emission), gain 110. For segmentation, YFP excitation was performed at 514 nm wavelength (laser intensity 3%) and the emission was collected at 525 to 560 nm, gain 110. Imaging processing and analysis were performed with FRETENATOR plugins (Rowe et al. 2022, 2023). The AxAm channel was used for segmentation. For segmentation, Otsu thresholds were used, a difference of Gaussian kernel size was determined empirically, and a minimum region of interest (ROI) size was set to 20. Distance from meristem was defined using FRETENATOR ROI labeler.

Jasmonate quantification

For hormone-level determination, dark-grown seedlings were harvested 2 d after germination, homogenized with mortar and pestle in liquid nitrogen, and reweighted into 3 replicates (approximately 10 mg per sample). Analysis of jasmonates was performed following a previously described protocol (Floková et al. 2014). Briefly, the samples were extracted in 1 mL of ice-cold 10% (v/v) aqueous methanol with the addition of isotopically labeled internal standards (JA-d_6 and JA-d_2-Ile, purchased from OlChemIm, Czech Republic), and the resulting extracts were purified on Oasis HLB SPE columns (1 cc/30 mg, Waters, Milford, MA, USA). The analyses were carried out using a 1290 Infinity liquid chromatography system coupled to an Agilent 6490 Triple Quadrupole mass spectrometer (Agilent Technologies, Santa Clara, CA, USA). The data were processed in MassHunter Quantitative B.09.00 software (Agilent Technologies, Santa Clara, CA, USA; Široká et al. 2022).

Accession numbers

The Arabidopsis Genome Initiative numbers for the genes mentioned in this article are as follows: AT1G78240 (*QUA2*); AT4G37580 (*HLS1*); AT2G43010 (*PIF4*); AT1G15550 (*GA3ox1*); AT4G25420 (*GA20ox1*); AT3G51160 (*MUR1*); AT1G30620 (*MUR4*); AT4G30440 (GAE1); AT3G23820 (*GAE6*); AT5G64740 (PRC1); AT5G49720 (*KOR1*); AT2G46370 (*JAR1*); AT2G39940 (*COI1*); AT2G01570 (RGA); AT1G14920 (*GAI*); AT1G66350 (*RGL1*); AT3G03450 (*RGL2*); AT5G17490 (*RGL3*); AT1G78440 (*GA2OX1*); AT1G30040 (*GA2OX2*); AT2G34555 (*GA2OX3*); AT1G47990 (*GA2OX4*); AT1G02400 (*GA2OX6*); AT1G50960 (*GA2OX7*); AT4G21200 (*GA2OX8*); and AT5G54380 (*THE1*).

Acknowledgments

We are grateful to Christian Fankhauser (University of Lausanne) for providing *PIF4p:PIF4-HApif4-301* seeds, to Edward Farmer (University of Lausanne) for providing *coi1-1* and *jar1-1* seeds, and to Shangwei Zhong (Peking University) for providing 35S:Myc-HLS1/*hls1-1* seeds. The authors acknowledge the facilities and technical assistance of the Umeå Plant Science Centre (UPSC) microscopy facility.

Author contributions

R.L. and S.F designed the project. R.L., Ö.E., K.J., D.T., Sa.R., J.G., and J.Š. performed experiments. R.L, S.F., S.V., S.R., A.M.J., and K.J. analyzed data and critically discussed results. S.F., S.V., S.R., K.J., O.N., and A.M.J. acquired the funding. R.L and S.F. wrote the manuscript together with contributions from all authors.

Supplementary data

The following materials are available in the online version of this article.

Supplementary Figure S1. Apical hook angle in pectin mutants grown on LA and HA.

Supplementary Figure S2. Osmotic support suppresses apical hook defects in pectin mutants.

Supplementary Figure S3. Effects of isx on the expression of genes involved in GA metabolism.

Supplementary Table S1. Primers used for RT-qPCR analysis and genotyping.

Funding

This work was supported by Sapienza University of Rome ("Progetti di Avvio alla Ricerca 2021—Tipo 2" grant no. AR22117A5E76C7EE, awarded to R.L.; "Progetti di Ricerca 2021—Progetti Medi" grant no. RM12218161B8A750 and Progetti di Ricerca 2019—Progetti Medi" grant no. RM11916B6F156C03, awarded to S.F.) and by Regione Lazio (grant no. A0375-2020-36720 "Alternative use of agri-food waste in a circular economy context," call Lazioinnova for Research Group Projects 2020, awarded to S.F.). This work was also supported by grants from the Knut and Alice Wallenberg Foundation (KAW 2016.0341, KAW 2016.0352, and KAW 2022.0029 [Sa.R.]), the Swedish Governmental Agency for Innovation Systems (VINNOVA 2016-00504), and Vetenskapsrådet VR-2020-03420 (Sa.R., S.R.). We also acknowledge the support of the Strategic Research Environment Bio4Energy, supported through the Swedish Government's Strategic Research Area initiative, for supporting this work. R.L. is supported by the Italian Ministry of University and Research (MUR) (project "Development of bio-based solutions for the valorisation of waste agri-food biomass," D.M. no. 1062-10.08.2021 PON "Ricerca e Innovazione" 2014-2020, Asse IV "Istruzione e ricerca per il recupero"—Azione IV.4—"Dottorati e contratti di ricerca su tematiche

dell'innovazione" e Azione IV.6—"Contratti di ricerca su tematiche Green"). J.Š. was financially supported by Czech Science Foundation project no. 22-17435S. J.Š. and O.N. thank Miroslava Špičáková for her technical support. D.T. is grateful for the technical assistance of Renata Plotzova and for financial support from the Ministry of Education, Youth and Sports of the Czech Republic (European Regional Development Fund-Project "Towards Next Generation Crops" no. CZ.02.01.01/00/22_008/0004581). J.G. and A.M.J. were supported by the Gatsby Charitable trust (GAT3395) and the European Research Council under the European Union's Horizon 2020 research and innovation program (grant agreement no. 759282). K.J. was supported by an international post-doc grant from Vetenskapsrådet (2020-06442). This study was carried out within the Agritech National Research Center and received funding from the European Union Next-GenerationEU (PIANO NAZIONALE DI RIPRESA E RESILIENZA (PNRR)—MISSIONE 4 COMPONENTE 2, INVESTIMENTO 1.4—D.D. 1032 17/06/2022, CN00000022). This manuscript reflects only the authors' views and opinions; neither the European Union nor the European Commission can be considered responsible for them.

Conflict of interest statement. None declared.

Data availability

The data underlying this article will be shared on reasonable request to the corresponding author.

References

Abbas M, Alabadí D, Blázquez MA. Differential growth at the apical hook: all roads lead to auxin. *Front Plant Sci*. 2013:4:441. https://doi.org/10.3389/fpls.2013.00441

An F, Zhang X, Zhu Z, Ji Y, He W, Jiang Z, Li M, Guo H. Coordinated regulation of apical hook development by gibberellins and ethylene in etiolated Arabidopsis seedlings. *Cell Res*. 2012:22(5):915–927. https://doi.org/10.1038/cr.2012.29

Aryal B, Jonsson K, Baral A, Sancho-Andres G, Routier-Kierzkowska A-L, Kierzkowski D, Bhalerao RP. Interplay between cell wall and auxin mediates the control of differential cell elongation during apical hook development. *Curr Biol*. 2020:30(9):1733–1739.e3. https://doi.org/10.1016/j.cub.2020.02.055

Bacete L, Hamann T. The role of mechanoperception in plant cell wall integrity maintenance. *Plants*. 2020:9(5):574. https://doi.org/10.3390/plants9050574

Bacete L, Schulz J, Engelsdorf T, Bartosova Z, Vaahtera L, Yan G, Gerhold JM, Tichá T, Øvstebø C, Gigli-Bisceglia N, *et al*. THESEUS1 modulates cell wall stiffness and abscisic acid production in *Arabidopsis thaliana*. *Proc Natl Acad Sci U S A*. 2022:119(1):e2119258119. https://doi.org/10.1073/pnas.2119258119

Baral A, Aryal B, Jonsson K, Morris E, Demes E, Takatani S, Verger S, Xu T, Bennett M, Hamant O, *et al*. External mechanical cues reveal a katanin-independent mechanism behind auxin-mediated tissue bending in plants. *Dev Cell*. 2021:56(1):67–80.e3. https://doi.org/10.1016/j.devcel.2020.12.008

Barbier de Reuille P, Routier-Kierzkowska A-L, Kierzkowski D, Bassel GW, Schüpbach T, Tauriello G, Bajpai N, Strauss S, Weber A, Kiss A, *et al*. MorphoGraphX: a platform for quantifying morphogenesis in 4D. *eLife*. 2015:4:05864. https://doi.org/10.7554/eLife.05864

Bethke G, Thao A, Xiong G, Li B, Soltis NE, Hatsugai N, Hillmer RA, Katagiri F, Kliebenstein DJ, Pauly M. Pectin biosynthesis is critical for cell wall integrity and immunity in *Arabidopsis thaliana*. *Plant Cell*. 2016:28(2):537–556. https://doi.org/10.1105/tpc.15.00404

Bonin CP, Potter I, Vanzin GF, Reiter W-D. The MUR1 gene of *Arabidopsis thaliana* encodes an isoform of GDP-d-mannose-4,6-dehydratase, catalyzing the first step in the de novo synthesis of GDP-l-fucose. *Proc Natl Acad Sci USA*. 1997:94(5):2085–2090. https://doi.org/10.1073/pnas.94.5.2085

Bouton S, Leboeuf E, Mouille G, Leydecker M-T, Talbotec J, Granier F, Lahaye M, Höfte H, Truong H-N. QUASIMODO1 encodes a putative membrane-bound glycosyltransferase required for normal pectin synthesis and cell adhesion in Arabidopsis. *Plant Cell*. 2002:14(10):2577–2590. https://doi.org/10.1105/tpc.004259

Burget EG, Verma R, Molhoj M, Reiter WD. The biosynthesis of L-arabinose in plants: molecular cloning and characterization of a Golgi-localized UDP-d-xylose 4-epimerase encoded by the MUR4 gene of Arabidopsis. *Plant Cell*. 2003:15(2):523–531. https://doi.org/10.1105/tpc.008425

Cosgrove DJ. Growth of the plant cell wall. *Nat Rev Mol Cell Biol*. 2005:6(11):850. https://doi.org/10.1038/nrm1746

de Lucas M, Davière J-M, Rodríguez-Falcón M, Pontin M, Iglesias-Pedraz JM, Lorrain S, Fankhauser C, Blázquez MA, Titarenko E, Prat S. A molecular framework for light and gibberellin control of cell elongation. *Nature*. 2008:451(7177):480–484. https://doi.org/10.1038/nature06520

Desnos T, Orbovic V, Bellini C, Kronenberger J, Caboche M, Traas J, Hofte H. Procuste1 mutants identify two distinct genetic pathways controlling hypocotyl cell elongation, respectively in dark-and light-grown Arabidopsis seedlings. *Development*. 1996:122(2):683–693. https://doi.org/10.1242/dev.122.2.683

Desprez T, Vernhettes S, Fagard M, Refrégier G, Desnos T, Aletti E, Py N, Pelletier S, Höfte H. Resistance against herbicide isoxaben and cellulose deficiency caused by distinct mutations in same cellulose synthase isoform CESA6. *Plant Physiol*. 2002:128(2):482–490. https://doi.org/10.1104/pp.010822

Du J, Kirui A, Huang S, Wang L, Barnes WJ, Kiemle SN, Zheng Y, Rui Y, Ruan M, Qi S, *et al*. Mutations in the pectin methyltransferase QUASIMODO2 influence cellulose biosynthesis and wall integrity in Arabidopsis. *Plant Cell*. 2020:32(11):3576–3597. https://doi.org/10.1105/tpc.20.00252

Engelsdorf T, Gigli-Bisceglia N, Veerabagu M, McKenna JF, Vaahtera L, Augstein F, Van der Does D, Zipfel C, Hamann T. The plant cell wall integrity maintenance and immune signaling systems cooperate to control stress responses in *Arabidopsis thaliana*. *Sci Signal*. 2018:11(536):eaao3070. https://doi.org/10.1126/scisignal.aao3070

Fagard M, Desnos T, Desprez T, Goubet F, Refregier G, Mouille G, McCann M, Rayon C, Vernhettes S, Höfte H. PROCUSTE1 encodes a cellulose synthase required for normal cell elongation specifically in roots and dark-grown hypocotyls of Arabidopsis. *Plant Cell*. 2000:12(12):2409–2424. https://doi.org/10.1105/tpc.12.12.2409

Feng S, Martinez C, Gusmaroli G, Wang Y, Zhou J, Wang F, Chen L, Yu L, Iglesias-Pedraz JM, Kircher S, *et al*. Coordinated regulation of *Arabidopsis thaliana* development by light and gibberellins. *Nature*. 2008:451(7177):475–479. https://doi.org/10.1038/nature06448

Feng W, Kita D, Peaucelle A, Cartwright HN, Doan V, Duan Q, Liu M-C, Maman J, Steinhorst L, Schmitz-Thom I. The FERONIA receptor kinase maintains cell-wall integrity during salt stress through Ca2+ signaling. *Curr Biol*. 2018:28(5):666–675.e5. https://doi.org/10.1016/j.cub.2018.01.023

Ferrari S, Galletti R, Vairo D, Cervone F, De Lorenzo G. Antisense expression of the *Arabidopsis thaliana* AtPGIP1 gene reduces polygalacturonase-inhibiting protein accumulation and enhances susceptibility to *Botrytis cinerea*. *Mol Plant Microbe Interact*. 2006:19(8):931–936. https://doi.org/10.1094/MPMI-19-0931

Floková K, Tarkowská D, Miersch O, Strnad M, Wasternack C, Novák O. UHPLC–MS/MS based target profiling of stress-induced

phytohormones. *Phytochemistry*. 2014:105:147–157. https://doi.org/10.1016/j.phytochem.2014.05.015

Franklin KA, Lee SH, Patel D, Kumar SV, Spartz AK, Gu C, Ye S, Yu P, Breen G, Cohen JD, *et al*. PHYTOCHROME-INTERACTING FACTOR 4 (PIF4) regulates auxin biosynthesis at high temperature. *Proc Natl Acad Sci USA*. 2011:108(50):20231–20235. https://doi.org/10.1073/pnas.1110682108

Freshour G, Bonin CP, Reiter W-D, Albersheim P, Darvill AG, Hahn MG. Distribution of fucose-containing xyloglucans in cell walls of the mur1 mutant of Arabidopsis. *Plant Physiol*. 2003:131(4):1602–1612. https://doi.org/10.1104/pp.102.016444

Griffiths J, Rizza A, Tang B, Frommer WB, Jones AM. Gibberellin perception sensors 1 and 2 reveal cellular GA dynamics articulated by COP1 and GA20ox1 that are necessary but not sufficient to pattern hypocotyl cell elongation. *bioRxiv* 2023.11.06.565859. 2023. https://doi.org/10.1101/2023.11.06.565859

Guzmán P, Ecker JR. Exploiting the triple response of Arabidopsis to identify ethylene-related mutants. *Plant Cell*. 1990:2(6):513–523. https://doi.org/10.1105/tpc.2.6.513

Hamann T, Bennett M, Mansfield J, Somerville C. Identification of cell-wall stress as a hexose-dependent and osmosensitive regulator of plant responses. *Plant J*. 2009:57(6):1015–1026. https://doi.org/10.1111/j.1365-313X.2008.03744.x

Hedden P, Phillips AL. Gibberellin metabolism: new insights revealed by the genes. *Trends Plant Sci*. 2000:5(12):523–530. https://doi.org/10.1016/S1360-1385(00)01790-8

Heim DR, Skomp JR, Tschabold EE, Larrinua IM. Isoxaben inhibits the synthesis of acid insoluble cell wall materials in *Arabidopsis thaliana*. *Plant Physiol*. 1990:93(2):695–700. https://doi.org/10.1104/pp.93.2.695

Heisler MG, Ohno C, Das P, Sieber P, Reddy GV, Long JA, Meyerowitz EM. Patterns of auxin transport and gene expression during primordium development revealed by live imaging of the Arabidopsis inflorescence meristem. *Curr Biol*. 2005:15(21):1899–1911. https://doi.org/10.1016/j.cub.2005.09.052

Hématy K, Sado P-E, Van Tuinen A, Rochange S, Desnos T, Balzergue S, Pelletier S, Renou J-P, Höfte H. A receptor-like kinase mediates the response of Arabidopsis cells to the inhibition of cellulose synthesis. *Curr Biol*. 2007:17(11):922–931. https://doi.org/10.1016/j.cub.2007.05.018

Jonsson K, Hamant O, Bhalerao RP. Plant cell walls as mechanical signaling hubs for morphogenesis. *Curr Biol*. 2022:32(7):R334–R340. https://doi.org/10.1016/j.cub.2022.02.036

Jonsson K, Lathe RS, Kierzkowski D, Routier-Kierzkowska A-L, Hamant O, Bhalerao RP. Mechanochemical feedback mediates tissue bending required for seedling emergence. *Curr Biol*. 2021:31(6):1154–1164.e3. https://doi.org/10.1016/j.cub.2020.12.016

Krupková E, Immerzeel P, Pauly M, Schmülling T. The TUMOROUS SHOOT DEVELOPMENT2 gene of Arabidopsis encoding a putative methyltransferase is required for cell adhesion and co-ordinated plant development. *Plant J*. 2007:50(4):735–750. https://doi.org/10.1111/j.1365-313X.2007.03123.x

Lehman A, Black R, Ecker JR. HOOKLESS1, an ethylene response gene, is required for differential cell elongation in the Arabidopsis hypocotyl. *Cell*. 1996:85(2):183–194. https://doi.org/10.1016/S0092-8674(00)81095-8

Li H, Johnson P, Stepanova A, Alonso JM, Ecker JR. Convergence of signaling pathways in the control of differential cell growth in Arabidopsis. *Dev Cell*. 2004:7(2):193–204. https://doi.org/10.1016/j.devcel.2004.07.002

Li K, Yu R, Fan L-M, Wei N, Chen H, Deng XW. DELLA-mediated PIF degradation contributes to coordination of light and gibberellin signalling in Arabidopsis. *Nat Commun*. 2016:7(1):11868. https://doi.org/10.1038/ncomms11868

Lin W, Tang W, Pan X, Huang A, Gao X, Anderson CT, Yang Z. Arabidopsis pavement cell morphogenesis requires FERONIA binding to pectin for activation of ROP GTPase signaling. *Curr Biol*. 2022:32(3):497–507.e4. https://doi.org/10.1016/j.cub.2021.11.030

Lorrai R, Ferrari S. Host cell wall damage during pathogen infection: mechanisms of perception and role in plant-pathogen interactions. *Plants*. 2021:10(2):399. https://doi.org/10.3390/plants10020399

Merz D, Richter J, Gonneau M, Sanchez-Rodriguez C, Eder T, Sormani R, Martin M, Hématy K, Höfte H, Hauser M-T. T-DNA alleles of the receptor kinase THESEUS1 with opposing effects on cell wall integrity signaling. *J Exp Bot*. 2017:68(16):4583–4593. https://doi.org/10.1093/jxb/erx263

Mielke S, Zimmer M, Meena MK, Dreos R, Stellmach H, Hause B, Voiniciuc C, Gasperini D. Jasmonate biosynthesis arising from altered cell walls is prompted by turgor-driven mechanical compression. *Sci Adv*. 2021:7(7):eabf0356. https://doi.org/10.1126/sciadv.abf0356

Mølhøj M, Verma R, Reiter W-D. The biosynthesis of d-galacturonate in plants. Functional cloning and characterization of a membrane-anchored UDP-d-glucuronate 4-epimerase from Arabidopsis. *Plant Physiol*. 2004:135(3):1221–1230. https://doi.org/10.1104/pp.104.043745

Mouille G, Ralet M-C, Cavelier C, Eland C, Effroy D, Hématy K, McCartney L, Truong HN, Gaudon V, Thibault J-F. Homogalacturonan synthesis in *Arabidopsis thaliana* requires a Golgi-localized protein with a putative methyltransferase domain. *Plant J*. 2007:50(4):605–614. https://doi.org/10.1111/j.1365-313X.2007.03086.x

Nicol F, His I, Jauneau A, Vernhettes S, Canut H, Höfte H. A plasma membrane-bound putative endo-1,4-β-d-glucanase is required for normal wall assembly and cell elongation in Arabidopsis. *EMBO J*. 1998:17(19):5563–5576. https://doi.org/10.1093/emboj/17.19.5563

Pfaffl MW. A new mathematical model for relative quantification in real-time RT–PCR. *Nucleic Acids Res*. 2001:29(9):e45. https://doi.org/10.1093/nar/29.9.e45

Raggi S, Ferrarini A, Delledonne M, Dunand C, Ranocha P, De Lorenzo G, Cervone F, Ferrari S. The Arabidopsis class III peroxidase AtPRX71 negatively regulates growth under physiological conditions and in response to cell wall damage. *Plant Physiol*. 2015:169(4):2513–2525. https://doi.org/10.1104/pp.15.01464

Ray PM, Green PB, Cleland R. Role of turgor in plant cell growth. *Nature*. 1972:239(5368):163–164. https://doi.org/10.1038/239163a0

Rayon C, Cabanes-Macheteau M, Loutelier-Bourhis C, Salliot-Maire I, Lemoine J, Reiter W-D, Lerouge P, Faye L. Characterization of N-glycans from Arabidopsis. Application to a fucose-deficient mutant1. *Plant Physiol*. 1999:119(2):725–734. https://doi.org/10.1104/pp.119.2.725

Reiter W-D, Chapple CC, Somerville CR. Altered growth and cell walls in a fucose-deficient mutant of Arabidopsis. *Science*. 1993:261(5124):1032–1035. https://doi.org/10.1126/science.261.5124.1032

Reiter W-D, Chapple C, Somerville CR. Mutants of *Arabidopsis thaliana* with altered cell wall polysaccharide composition. *Plant J*. 1997:12(2):335–345. https://doi.org/10.1046/j.1365-313X.1997.12020335.x

Rizza A, Walia A, Lanquar V, Frommer WB, Jones AM. In vivo gibberellin gradients visualized in rapidly elongating tissues. *Nat Plants*. 2017:3(10):803–813. https://doi.org/10.1038/s41477-017-0021-9

Rouet M-A, Mathieu Y, Barbier-Brygoo H, Laurière C. Characterization of active oxygen-producing proteins in response to hypo-osmolarity in tobacco and Arabidopsis cell suspensions: identification of a cell wall peroxidase. *J Exp Bot*. 2006:57(6):1323–1332. https://doi.org/10.1093/jxb/erj107

Rowe J, Grangé-Guermente M, Exposito-Rodriguez M, Wimalasekera R, Lenz MO, Shetty KN, Cutler SR, Jones AM. Next-generation ABACUS biosensors reveal cellular ABA dynamics driving root growth at low aerial humidity. *Nat Plants*. 2023:9(7):1103–1115. https://doi.org/10.1038/s41477-023-01447-4

Rowe JH, Rizza A, Jones AM. Quantifying phytohormones in vivo with FRETFörster resonance energy transfer (FRET) BiosensorsBiosensors and the FRETENATOR analysis toolset. In: Duque P, Szakonyi D, editors. *Environmental responses in plants: methods and protocols*. New York (NY): Springer US; 2022. p. 239–253.

Rui Y, Dinneny JR. A wall with integrity: surveillance and maintenance of the plant cell wall under stress. *New Phytol*. 2020:225(4):1428–1439. https://doi.org/10.1111/nph.16166

Shen X, Li Y, Pan Y, Zhong S. Activation of HLS1 by mechanical stress via ethylene-stabilized EIN3 is crucial for seedling soil emergence. *Front Plant Sci*. 2016:7:1571. https://doi.org/10.3389/fpls.2016.01571

Silk WK, Erickson RO. Kinematics of hypocotyl curvature. *Am J Bot*. 1978:65(3):310–319. https://doi.org/10.1002/j.1537-2197.1978.tb06072.x

Sinclair SA, Larue C, Bonk L, Khan A, Castillo-Michel H, Stein RJ, Grolimund D, Begerow D, Neumann U, Haydon MJ, *et al.* Etiolated seedling development requires repression of photomorphogenesis by a small cell-wall-derived dark signal. *Curr Biol*. 2017:27(22):3403–3418.e7. https://doi.org/10.1016/j.cub.2017.09.063

Široká J, Brunoni F, Pěnčík A, Mik V, Žukauskaitė A, Strnad M, Novák O, Floková K. High-throughput interspecies profiling of acidic plant hormones using miniaturised sample processing. *Plant Methods*. 2022:18(1):122. https://doi.org/10.1186/s13007-022-00954-3

Song S, Huang H, Gao H, Wang J, Wu D, Liu X, Yang S, Zhai Q, Li C, Qi T, *et al.* Interaction between MYC2 and ETHYLENE INSENSITIVE3 modulates antagonism between jasmonate and ethylene signaling in Arabidopsis. *Plant Cell*. 2014:26(1):263–279. https://doi.org/10.1105/tpc.113.120394

Sun T. Gibberellin metabolism, perception and signaling pathways in Arabidopsis. *Arabidopsis Book*. 2008:6:e0103. https://doi.org/10.1199/tab.0103

Vaahtera L, Schulz J, Hamann T. Cell wall integrity maintenance during plant development and interaction with the environment. *Nat Plants*. 2019:5(9):924–932. https://doi.org/10.1038/s41477-019-0502-0

Verger S, Long Y, Boudaoud A, Hamant O. A tension-adhesion feedback loop in plant epidermis. *Elife*. 2018:7:e34460. https://doi.org/10.7554/eLife.34460

Wasternack C, Hause B. Jasmonates: biosynthesis, perception, signal transduction and action in plant stress response, growth and development. An update to the 2007 review in annals of botany. *Ann Bot*. 2013:111(6):1021–1058. https://doi.org/10.1093/aob/mct067

Willis L, Refahi Y, Wightman R, Landrein B, Teles J, Huang KC, Meyerowitz EM, Jönsson H. Cell size and growth regulation in the *Arabidopsis thaliana* apical stem cell niche. *Proc Natl Acad Sci USA*. 2016:113(51):E8238–E8246. https://doi.org/10.1073/pnas.1616768113

Wolf S, Hématy K, Höfte H. Growth control and cell wall signaling in plants. *Annu Rev Plant Biol*. 2012:63(1):381–407. https://doi.org/10.1146/annurev-arplant-042811-105449

Zhang B, Holmlund M, Lorrain S, Norberg M, Bakó L, Fankhauser C, Nilsson O. BLADE-ON-PETIOLE proteins act in an E3 ubiquitin ligase complex to regulate PHYTOCHROME INTERACTING FACTOR 4 abundance. *eLife*. 2017:6:e26759. https://doi.org/10.7554/eLife.26759

Zhang X, Ji Y, Xue C, Ma H, Xi Y, Huang P, Wang H, An F, Li B, Wang Y, *et al.* Integrated regulation of apical hook development by transcriptional coupling of EIN3/EIL1 and PIFs in Arabidopsis. *Plant Cell*. 2018:30(9):1971–1988. https://doi.org/10.1105/tpc.18.00018

Zhang X, Zhu Z, An F, Hao D, Li P, Song J, Yi C, Guo H. Jasmonate-activated MYC2 represses ETHYLENE INSENSITIVE3 activity to antagonize ethylene-promoted apical hook formation in Arabidopsis. *Plant Cell*. 2014:26(3):1105–1117. https://doi.org/10.1105/tpc.113.122002